THE UNIVERSITY OF MICHIGAN

COLLEGE OF ENGINEERING

DEPARTMENT OF ELECTRICAL ENGINEERING

Radiation Laboratory

1082-3-Q = RL-2025

DOPPLER RADIATION STUDY

Quarterly Report No. 3

1 January 1968 - 1 April 1968

By

Chiao-Min Chu, Joseph E. Ferris and Andrew M. Lugg

April 1968

Contract No. N62269-67-C-0545

Contract With: The U. S. Naval Air Development Center
Johnsville, Warminster, PA. 18974

Administered through:

OFFICE OF RESEARCH ADMINISTRATION • ANN ARBOR

TABLE OF CONTENTS

ABSTRACT

In this, the Third Quarterly Report on "Doppler Radiation Study", some results of the theoretical investigation and details of the experimental efforts are reported.

Much of the experimental work is directed toward preparing the equipment which will be used during the forthcoming fly-by tests. The radar tracking, data collection and communication equipment has been checked out and is ready for the scheduled test.

In the theoretical study, the numerical calculation of the spatial and temporal variation of the reflected radiation from a perfectly conducting ground , based on the scheme suggested in the last quarterly report, has been carried out. Further, some simplifications in presentation of the numerical results by using nomographs are introduced. The reflected radiation due to a diffusely reflecting ground is determined numerically and in an approximate but closed form; and finally the effect of some meteorogical conditions, such as cloud reflection, and the variation of the refractive index of the atmosphere are also considered.

I

INTRODUCTION

This is the Third Quarterly Report on Contract N62269-67-C-0545, "Doppler Radiation Study". It covers the period 1 January to 1 April 1968.

The primary objective of this project is to characterize the radiation from airborne doppler navigational radar systems, and to determine the probability of detecting this radiation. The task is being carried out in the following phases:

1) Experimental measurement of the radiation patterns of several antennas that are currently being used in doppler navigational systems.

2) Based on the measure radiation pattern, the distribution of radiation in space and the effects due to ground reflection, airplane maneuvering, and meteorological conditions are investigated.

3) The theoretical results in (2) are to be checked out against results obtained from the flight test.

4) From the theoretical and experimental results, estimates of the probability of detecting the radiation at different ranges will be made.

During the present research period, the following has been accomplished:

1) The data collection, radar tracking, and communication equipment that is to be used in a fly-by test scheduled for April, 1968, have been checked out and are ready for operation.

2) Numerical computation of the radiation reflected by a perfectly conducting ground from an AN/APN-153 doppler antenna has been carried out, the results being presented in a compact, normalized form. Several nomographs are developed in conjunction with the computed data to facilitate the estimation of spatial and temporal variation of the reflected radiation for differing aircraft trajectories. The use of the computed data and monographs is illustrated and explained by means of examples.

3) Formulations and schemes for the calculation of radiation reflected from a diffusely reflecting ground are presented. Anticipating that narrow beams will be used in future doppler systems, an approximate formulation of the computation, in which the beam is assumed Gaussian, is also carried out.

4) An initial investigation of the effect of meteorological conditions on the propagation of radiation is outlined. The effect of a specularly reflecting overcast layer and the effect of a linearly varying refractive index of atmosphere with height, are considered.

Some of the results of the above investigations were included in the Memorandum 01082-508-M. For a coherent, integrated discussion of the problem, some of these results are also included in this report.

In the next research period, more numerical calculations involving a diffusely reflecting ground using finer increments of integration will be carried out to determine the effect of the fine structure of the measured radiation pattern. Numerical methods for investigating the effect of various meteorological conditions and maneuvering will also be developed, and the numerical results will be compared with the data obtained from the fly-by tests.

II

EXPERIMENTAL EFFORT

Much of the experimental effort during this period has been concentrated towards readying the radar site for the fly-by tests which are to be conducted in the early part of April. Preparation of the radar site has involved readying the following equipment:

1) Communication equipment,
2) Radar tracking equipment,
3) Data collection equipment,

The transmitter and receiver of the communication equipment have been checked out and are operating satisfactorily. During the fly-by tests a frequency of 248.3 MHz is to be employed for voice communication between the ground and air. The communication link will be required to maintain contact with the aircraft and as an aid in directing the aircraft's course. The communication equipment is compatible with the ARC-27. Its nomenclature is a GR-217 radio transmitter capable of transmitting 100 watts of RF power.

The radar system which will be employed during the fly-by tests is a NIKE missile system. The NIKE system consists of three radars; a missile tracking radar (X-band), target tracking radar (X-band), and a search radar (S-band). The missile tracking radar will be employed to track the aircraft during the fly-by tests. The target tracking radar will be slaved with the missile tracking radar, such that, during tracking, it will follow and point in the same direction as the missile tracking radar. Rather than using the receiver normally associated with the target tracking radar, a K_u-band horn antenna will be employed with a target tracking pedestal. In this configuration the horn will point toward the aircraft during the tests. Data collected by the K_u-band antenna will be transferred through a transmission cable to a laboratory receiver (a Micro-Tel Wide Range WR - 250

Receiver). In addition to the Wide Range Receiver, a small amplifier will be required at the output to further amplify the received signal from the doppler navigation system. The amplified signal is required for the data recording system. The S-band search radar will yield information of other aircraft in the area.

In the data recording system, we are employing two sub-systems. The first consists of an analog data system, the 4-channel Sanborn Recorder, and the second is a multi-channel digital system. The two sub-systems will be connected in parallel so that analog and digital data may be collected simultaneously. The following information is to be recorded during testing: the doppler navigation signal strength and the x, y and z coordinates of the aircraft (from the missile tracking radar) during the fly-by tests. In addition to the above data, we have the capability of collecting $\sin\theta$ and $\sin\phi$ information (from the target tracking radar) when making specular reflection measurements.

During the initial phase of the fly-by tests, data will be collected from the doppler system by pointing the tracking radar antenna with the K_u-band receiving system at the aircraft and by collecting the relative signal strength as a function of aircraft position. This data will be compared with predicted signal levels to confirm the feasibility of detecting the aircraft. During the second phase of the fly-by tests, efforts will be made to determine the probability of aircraft detection on the basis of specular reflections. These specular reflections will be assumed to occur as a result of the signals that may be reflected from the earth toward the radar or possibly specular reflections that are reflected from the earth up to the sky and re-reflected from clouds or other atmospheric phenomena.

III

THEORETICAL STUDY

3.1 Spatial Distribution of Specularly Reflected Radiation

The calculation of the component of radiation specularly reflected from the ground (assumed to be smooth, and perfectly conducting), by using geometrical optics, has been formulated and reported previously in Chu et al, (1968). In this quarter, the pertinent numerical calculation based on the measured radiation pattern of AN/APN-153 doppler antenna were carried out. Nomographs, reducing the actual geometrical distances between the antenna and the observer into a set of normalized coordinates are constructed. When these nomographs are used in conjunction with one set of calculated, reflected radiation data an estimation of the reflected radiation at different points of observation and under various flight trajectories of the vehicle carrying the doppler radar, can be found.

As reported previously, for an antenna at $T(x_a, y, z_a)$, and an observer at $B(x_h, y_h, h)$, as illustrated in Fig. 3-1, the calculation of the reflected radiation can be more conveniently carried out by introducing the normalized coordinates defined below:

$$\xi = \frac{z_a - h}{z_a + h} \tag{3.1}$$

$$X = \frac{x - x_a}{z_a} = -\frac{2}{1+\xi} \tan\theta \cos\phi \tag{3.2}$$

and

$$Y = \frac{y - y_a}{z_a} = -\frac{2}{1+\xi} \tan\theta \sin\phi \quad . \tag{3.3}$$

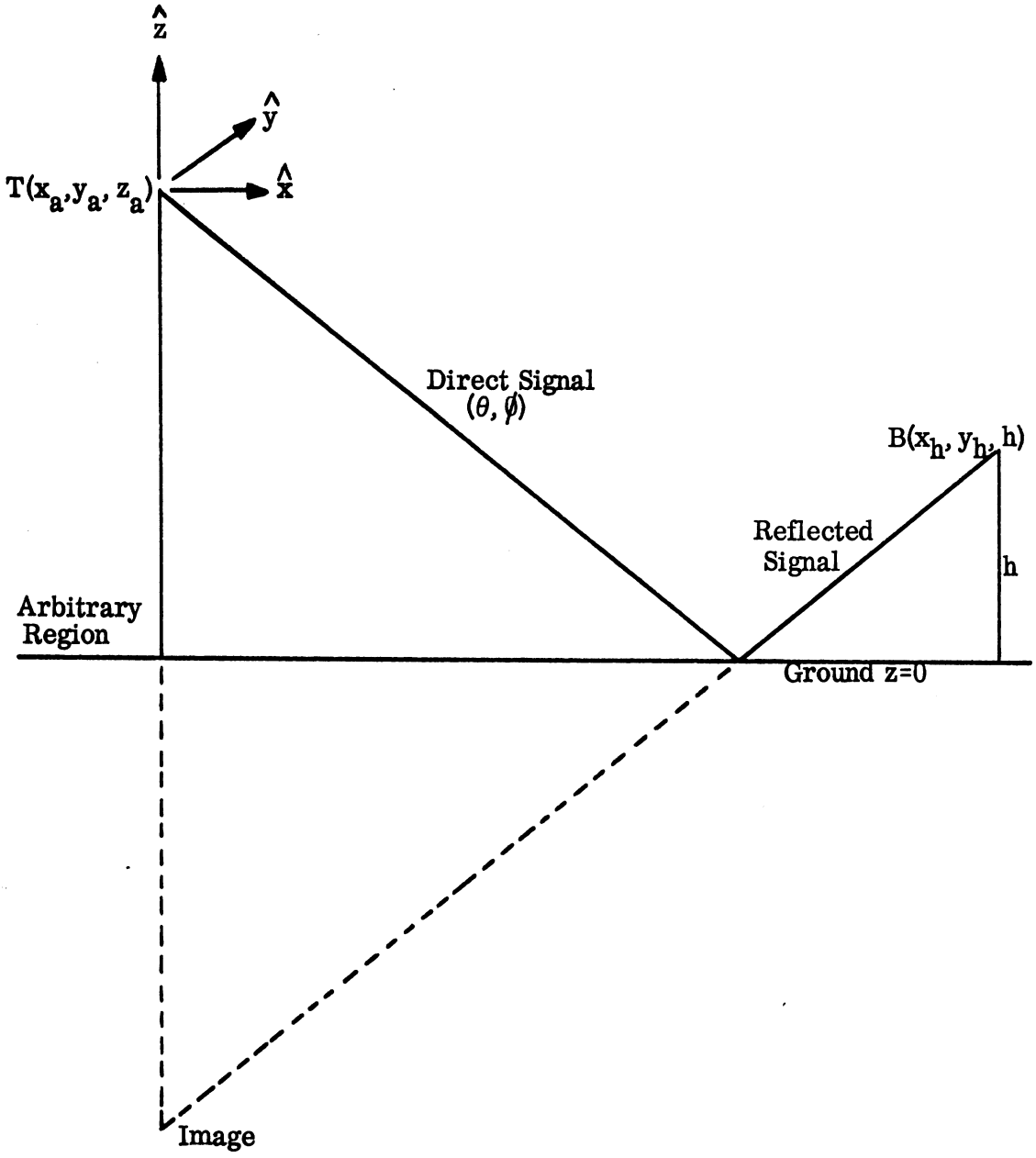

FIG. 3-1: GEOMETRY FOR REFLECTED RAY

The normalized coordinates can be expressed in terms of the values $(x - x_a)$, $(y - y_a)$, z_a and h. A nomograph has been constructed to link these two coordinate systems. It is given in Fig. 3-2.

Fig. 3-2 is a nomograph which relates the actual position of an observer (x, y, h) to the normalized position vector (X, Y, ξ). Here the initial aircraft position is $(x = x_a, y = y_a, z = z_a)$. An example, x = 5000 ft., y = 10,000 ft., z_a = 20,000 ft, h = 5000 ft. is given in Fig. 3-2 to illustrate the way the nomograph is to be used.

The procedure for finding X, Y, and ξ from the nomograph is as follows:

1) On the left hand axis mark $(x - x_a)$ or $(y - y_a)$ and on the center axis mark z_a. Where the lines joining these points intersect line A, mark off X or Y.

2) On the right hand axis mark h. Where the line joining z_a, on the center axis and h intersects line B, read off ξ.

Now, in terms of the normalized coordinates the intensity of the ground reflected radiation from an antenna with radiation pattern $f^2(\theta, \phi)$, power P_t and gain G_t is given by

$$P_r(X, Y, \xi) = \frac{P_t G_t f^2(\theta, \phi)}{z_a^2 \left(\frac{2}{1+\xi}\right)^2 \sec^2 \theta} \quad . \tag{3.4}$$

If we take the power level of the reflected radiation at any height of observation from the direction of maximum radiation as 0 db, then, the reflected radiation due to rays in any direction (θ, ϕ) is given by

$$db_r(\theta, \phi) = db_o(\theta, \phi) + 20 \log \sec \theta_M - 20 \log \sec \theta \tag{3.5}$$

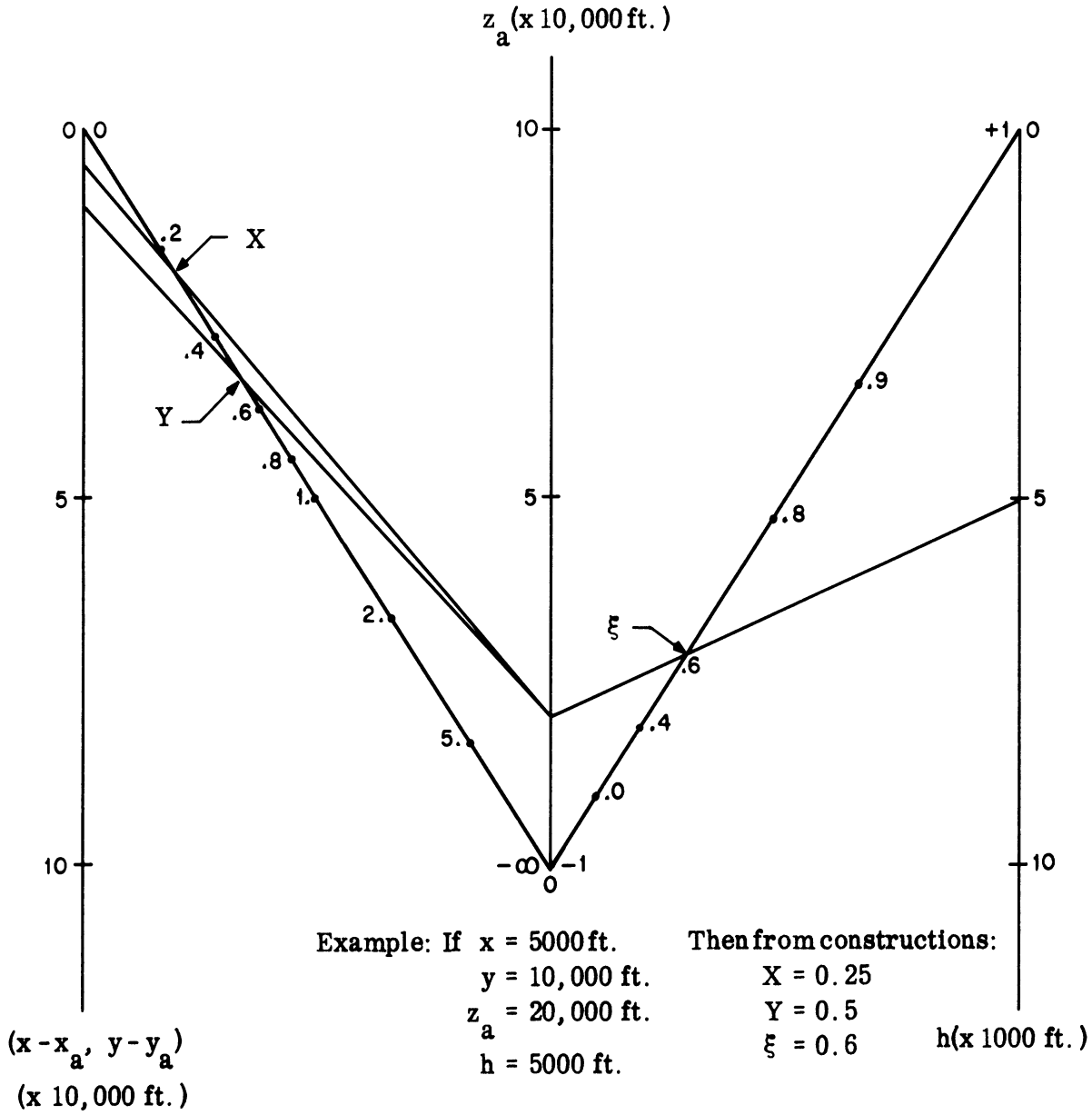

FIG. 3-2: NOMOGRAPH RELATING (x, y, h, z_a) to (X, Y, ξ).

where $db_o(\theta,\phi)$ is the measured radiation pattern and (θ_M, ϕ_M) is the direction of maximum radiation. Numerically, for each θ,ϕ, we may calculate $db_r(\theta,\phi)$, while for each θ, ϕ, ξ, we may compute a set of X and Y. It was suggested previously that contour plots for constant db_r in the X-Y-plane can be plotted for each ξ. However, an inspection of Eq. (3.2) and (3.3) reveals that for each θ, ϕ, the dependence of X, Y on ξ is simple. Thus, it is seen that one set of computation, relating db_r to the normalized coordinates X and Y for $\xi = 1$ is all that is required. For any other value of ξ, the same graph of the computational results may be used if we change the scale of X and Y. This change of scale is given by

$$X(\xi) = \frac{2}{1+\xi} X(\xi = 1) \tag{3.5}$$

and

$$Y(\xi) = \frac{2}{1+\xi} X(\xi = 1) \quad . \tag{3.6}$$

The transformation can be easily accomplished by the nomograph given in Fig. 3-3.

Figure 3-3 may be used in eactly the same was as the nomographs introduced above. For example suppose $h/z_a = .1$, $\xi = 0.817$. If we desire the position on the $X(\xi = 1)$, $Y(\xi = 1)$ scales for $X = 1$, $Y = 0.4$, we mark off 1 unit on the left hand scale and draw a line through this point and the point $\xi = 0.817$ on the ξ scale. Where this constructed line meets the right hand scale, $X(\xi = 1)$ is read off. In this case $X(\xi = 1) = 0.908$. Similarly when $Y = 0.4$; $Y(\xi = 1) = .363$.

In Figs. 3-4 and 3-5, a contour plot of db_r in the X-Y-plane for $\xi = 1$ is given. This one set of curves, as suggested above may be used for all values of ξ by changing of the scales of X and Y.

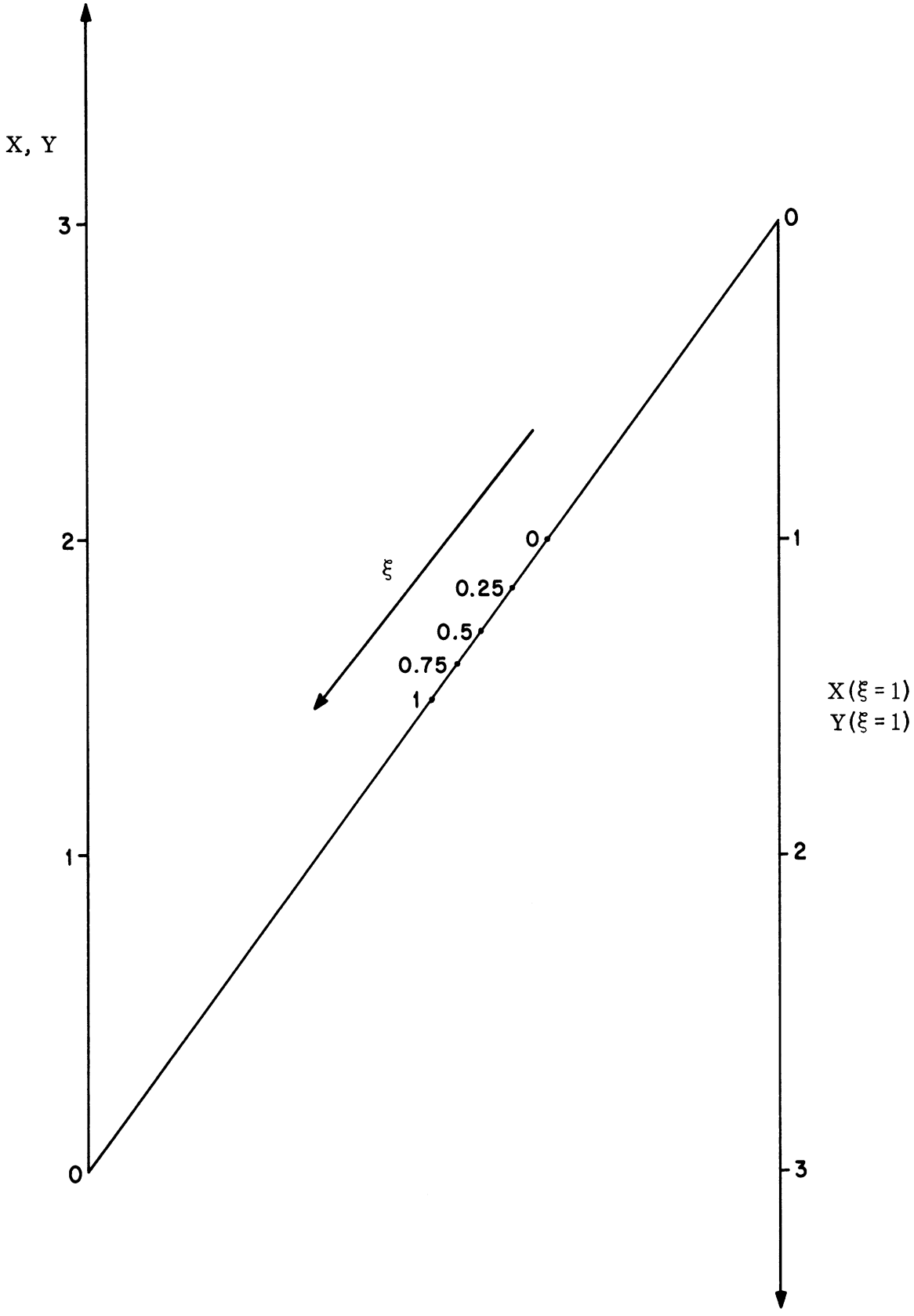

FIG. 3-3: NOMOGRAPH RELATING X, Y, ξ TO X(ξ = 1), Y(ξ = 1).

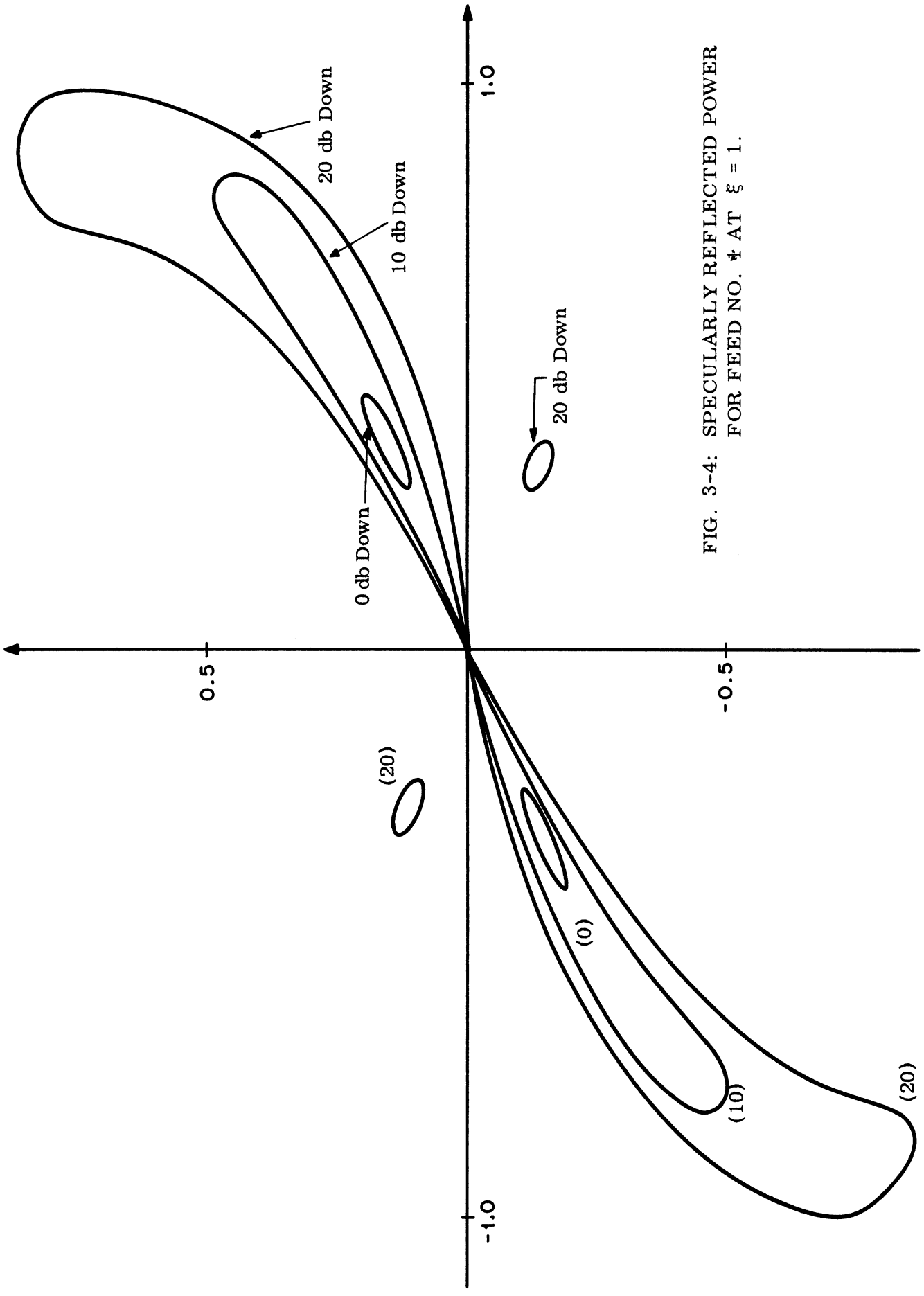

FIG. 3-4: SPECULARLY REFLECTED POWER FOR FEED NO. ϕ AT $\xi = 1$.

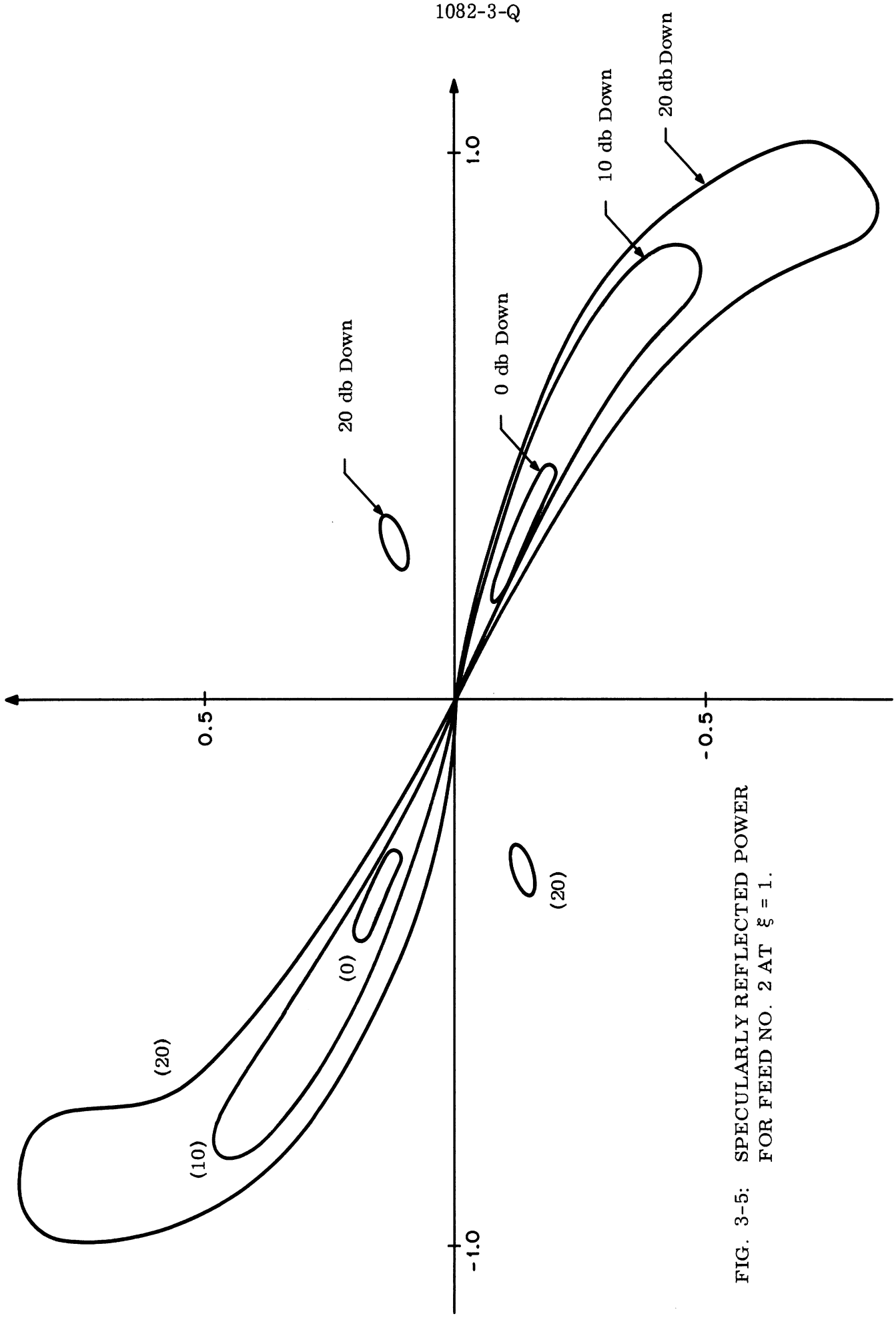

FIG. 3-5: SPECULARLY REFLECTED POWER FOR FEED NO. 2 AT $\xi = 1$.

For completeness, it is seen that given x, y, h and x_a, y_a, z_a, the ground reflection observed can be directly estimated by using the contour plots in Figs. 3-4 and 3-5. From Eqs. (3.1), (3.2) and (3.3), we have:

$$x - x_a = X(\xi = 1)\left[z_a + h\right] \tag{3.7}$$

$$y - y_a = Y(\xi = 1)\left[z_a + h\right] \quad . \tag{3.8}$$

These relations may be used to obtain the values of $X(\xi = 1)$, $Y(\xi = 1)$ directly for estimating the reflected radiation from Figs. 3-4 and 3-5. The necessary nomograph is given by Fig. 3-6.

It is to be noted that for the calculation of the specularly reflected radiation the use of Fig. 3-6 in conjunction with Fig. 3-4 and/or Fig. 3-5 will yield the required information. However, it is seen later in this report that, when using these computed results to estimate the temporal variation the reflected radiation, and when the case of a diffusely reflecting ground, is considered then $X(\xi)$ and $Y(\xi)$ are the more convenient normalizations.

3.2 Temporal Variation of Radiation Specularly Reflected from a Plane Ground

From the basic equation for the power level of the reflected radiation observed at any point,

$$db_r(\theta,\phi) = db_o(\theta,\phi) + 20 \log \frac{\sec\theta_M}{\sec\theta} \quad ,$$

and the graph of the variation of db_r with X and Y (Figs. 3-4 and 3-5), the temporal variation of the reflected radiation due to a pulsed source and a moving vehicle can be computed. The basic scheme for such a computation has been given in the previous report (Chu et al 1968). During this research period, this scheme has been applied to the AN/APN-153 antenna system for level flight of the vehicle.

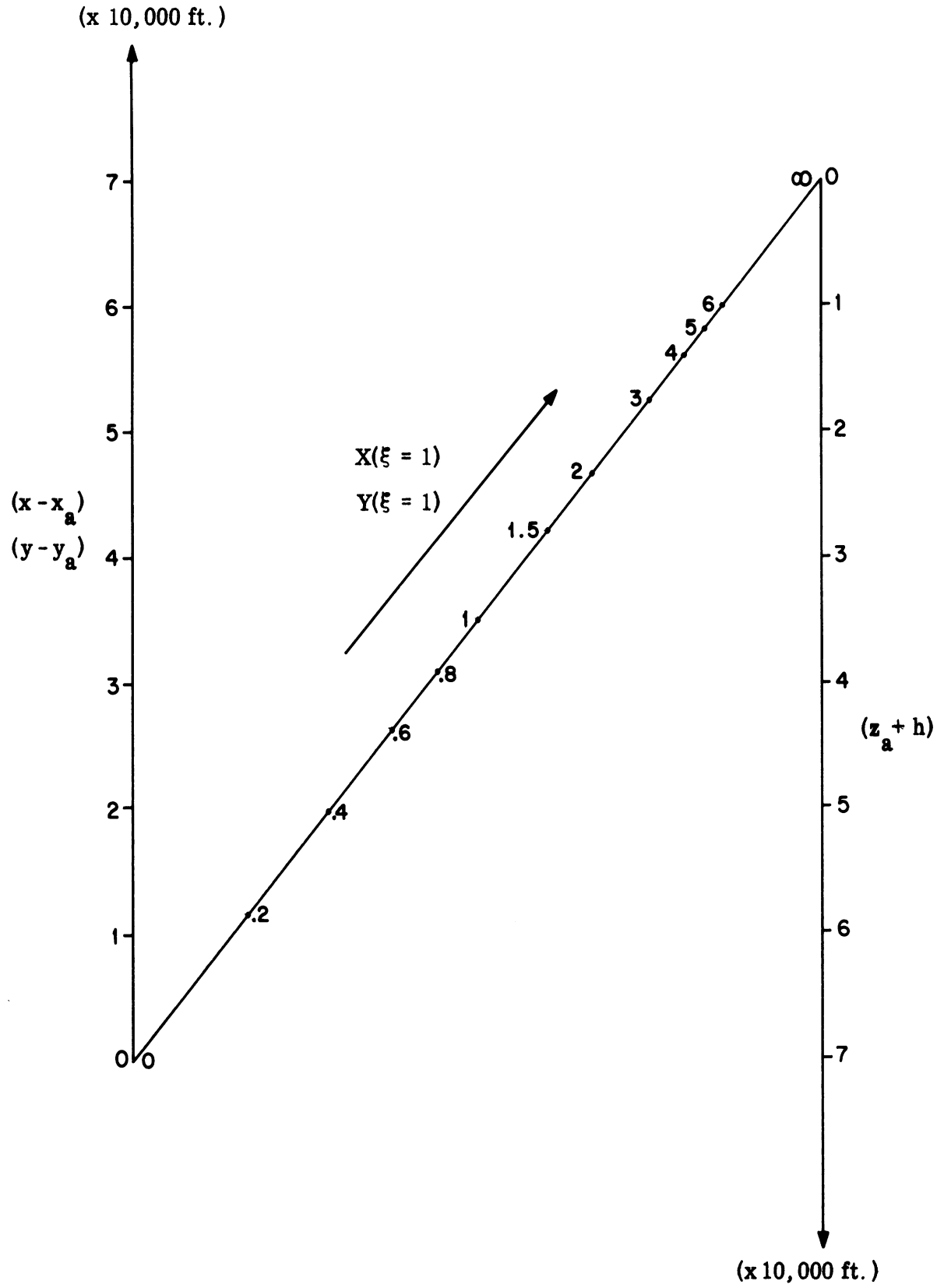

FIG. 3-6: NOMOGRAPH RELATING $(x - x_a)$, $(y - y_a)$, $(z_a + h)$ TO $X(\xi = 1)$, $Y(\xi = 1)$.

Basically, the temporal variation of the intensity of the reflected radiation is due to the following:

1) The modulation of the source,

2) The time delay depending on the time taken for the wave to propagate between the source and the observer. This delay, as mentioned in Chu et al, (1968), is given by

$$\tau = t - t_o = \frac{R'}{c} = \frac{z_a}{c}\sqrt{X^2 + Y^2 + \left(\frac{2}{1+\xi}\right)^2} \qquad (3.9)$$

3) The change of θ and ϕ which result from the aircraft motion.

As illustrated in Chu et al, (1968), for a moving vehicle with trajectory described by $x_a(t_o)$, $y_a(t_o)$, $z_a(t_o)$ and with radiating, time varying pulsed power , P(t) the intensity of radiation observed by a fixed observer is formally given by

$$P_r = \frac{P(t_o + \tau(t_o))\, G_t f^2(\theta(t_o), \phi(t_o)) \sec^2\theta_M}{4\pi z_a^2 \left[X^2(t_o) + Y^2(t_o) + \left(\frac{2}{1+\xi(t_o)}\right)^2\right] \sec^2\theta(t_o)} \quad . \qquad (3.10)$$

This formula indicates that the temporal variation of the intensity of the reflected radiation may be separated into two parts, the part $P(t_o + \tau(t_o))G_t$ depending on the form of the modulation of the antenna signal, and the term

$$M(t_o) = \frac{f^2(\theta(t_o), \phi(t_o))\, \sec^2\theta_M}{4\pi z_a^2 \left[X^2(t_o) + Y^2(t_o) + \left(\frac{2}{1+\xi(t_o)}\right)^2\right] \sec^2\theta(t_o)} \quad . \qquad (3.11)$$

For an aircraft flying at a fixed height, the variation of M with X, Y expressed in db relative to the maximum power level observable at that height may be plotted.

Thus, knowing the trajectory, the variation of $M(t_o)$ $\left[\text{given in terms } db(t_o)\right]$ with t_o can be calculated directly.

To illustrate this variation, we shall consider two cases for level flight of the airplane. For these cases z_a, and hence ξ are constant with respect to a fixed observer. The airplane is assumed to be moving with uniform velocity. For convenience, the normalized time scale

$$S_o = \frac{Vt_o}{z_a} \tag{3.12}$$

is also introduced.

For the first case, the airplane is taken to be flying parallel to the x-axis. The projections of airplane trajectory and observer on the ground are illustrated in Fig. 3-7. For this case, the normalized coordinate Y is not changed during flight. Furthermore, if we take $t_o = 0$ at the moment when the airplane is nearest to the observer (point A in Fig. 3-7), we find that

$$X(t_o) = \frac{Vt_o}{z_a} \triangleq S_o \tag{3.13}$$

Curves of $db_r(t_o)$ against t_o for $\xi = 1$, Feed No. 1, and several values of Y are given in Fig. 3-8.

It is seen from the Fig. 3-8 that when the aircraft pases overhead, the peaks are not aymmetrical and are well below the maximum power level. The received power in this case derives from the "fine structure". When the distance of closest approach is $Y_N = 0.15$, the received power goes through maxima at $S_o = 0.38$ and at $S_o = -0.4$. At the former normalized time the power received derives from the mainlobe and at $S_o = -0.4$ it derives from a sidelobe. As the distance of nearest approach increases the maxima decrease (see curve for $Y_N = 0.5$). The receiver, under this condition is picking up radiated power from the "edges" of the mainlobes and sidelobes.

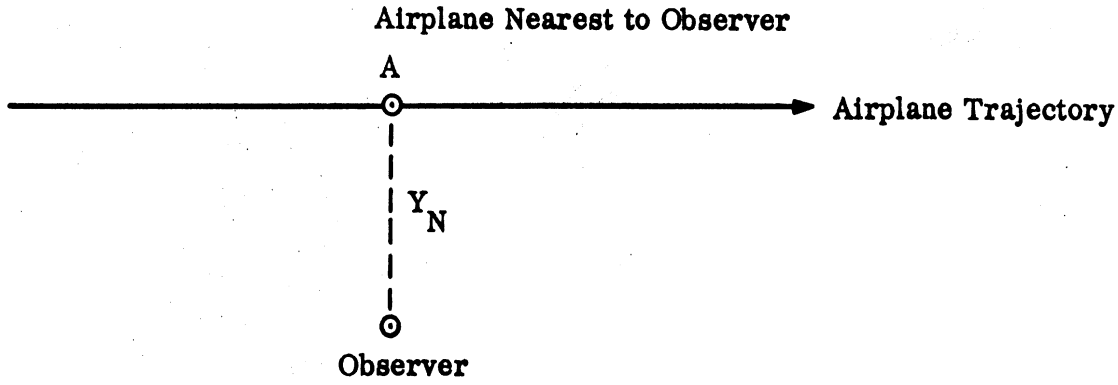

FIG. 3-7: GEOMETRY FOR AIRCRAFT FLYING AT A CONSTANT HEIGHT AND WITH $Y(\xi)$ = CONSTANT.

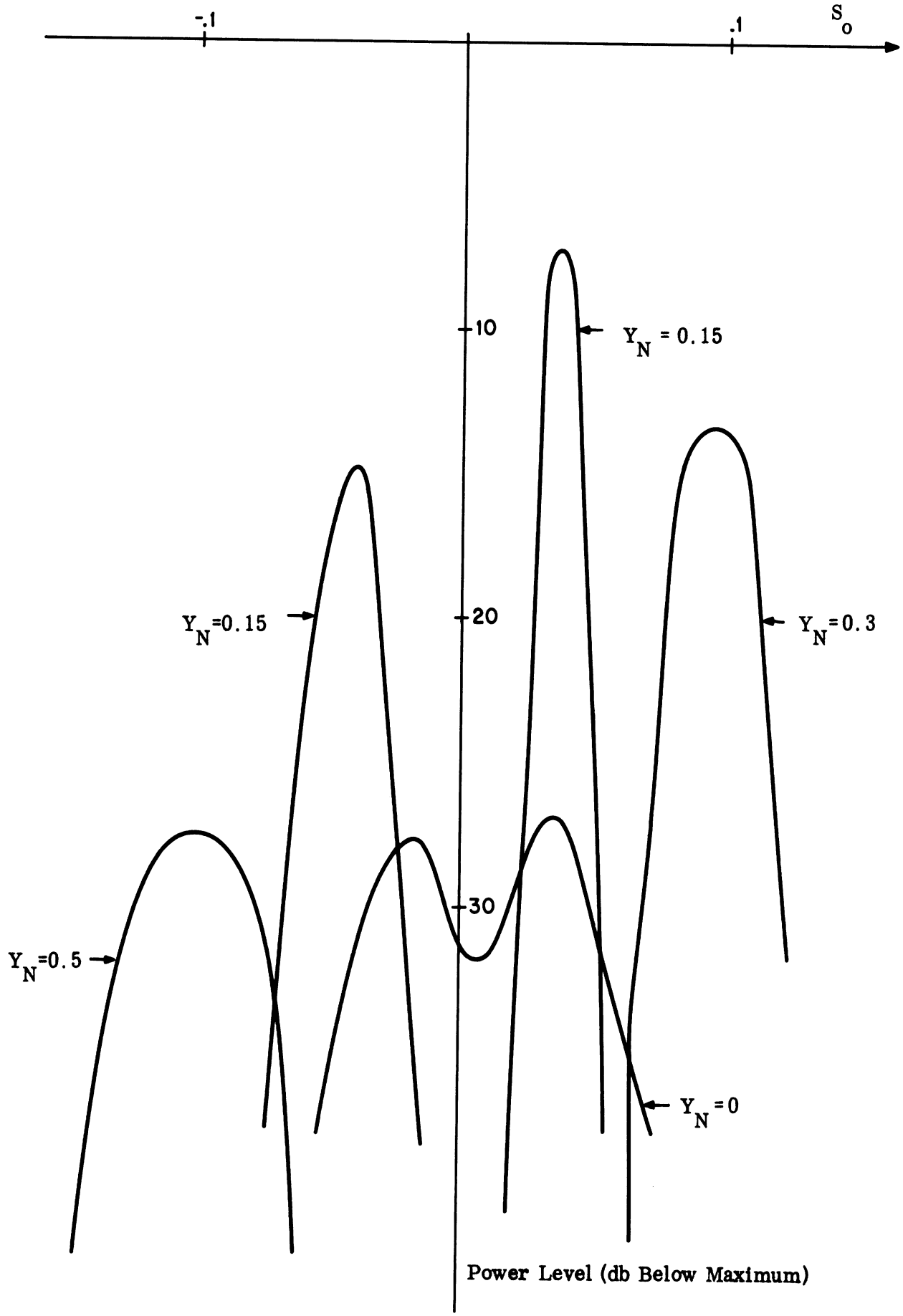

FIG. 3-8: RECEIVED POWER AGAINST NORMALIZED TIME FOR $X = 0$, $\xi = 1$ AND VARIOUS VALUES OF Y_N.

Also, it should be noted that at other heights ($\xi \neq 1$) these curves may also be used in conjunction with the nomograph given in Fig. 3-3 or Fig. 3-6. The resulting time scale change is directly proportional to change in the X scale given in the nomograph. The procedure for finding the time scale is as follows: use Fig. 3-3 or Fig. 3-6 to find the change in the X scale for the new height. This scale then becomes the new S_o scale. The plot of power level in db below maximum is now given against S_o for the required fixed height.

For the second illustrative case, let us consider an airplane flying with circular path, as illustrated by the ground projection in Fig. 3-9. If again, we choose $t_o = 0$ when the airplane is closest to the observation point (i.e. at point A in Fig. 3-9) we have at $t_o = 0$,

$$X(o) = 0$$

$$Y(o) = Y_o \quad .$$

If the radius of circling is $\rho (=R/z_a)$ then for any t_o, we have,

$$X(t_o) = -(\rho - Y_o) \sin\left(\frac{S_o}{\rho}\right)$$

and

$$Y(t_o) = \rho - (\rho - Y_o) \cos\left(\frac{S_o}{\rho}\right) \quad .$$

Numerical results for $\rho = 1$, and $Y_o = 0.1$ are presented in Fig. 3-10.

The time of the propagation for these cases can be also calculated. For the first case,

$$\tau(t_o) = \frac{z_a \sqrt{X(t_o)^2 + Y^2 + \left(\frac{2}{1+\xi}\right)^2}}{c} \quad . \tag{3.14}$$

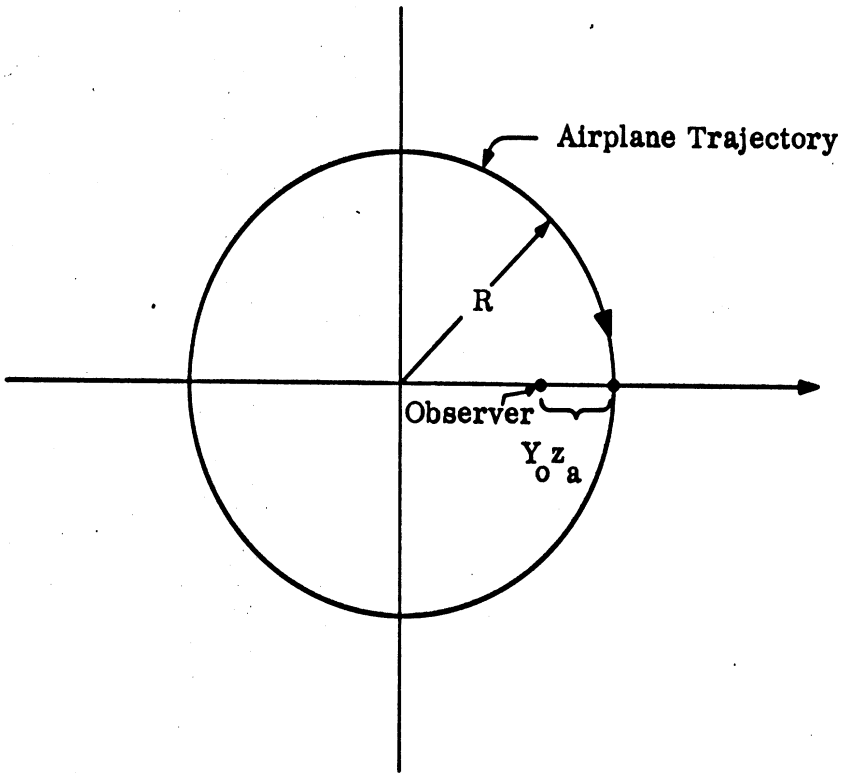

FIG. 3-9: GEOMETRY FOR AIRCRAFT CIRCLING WITH CONSTANT RADIUS R.

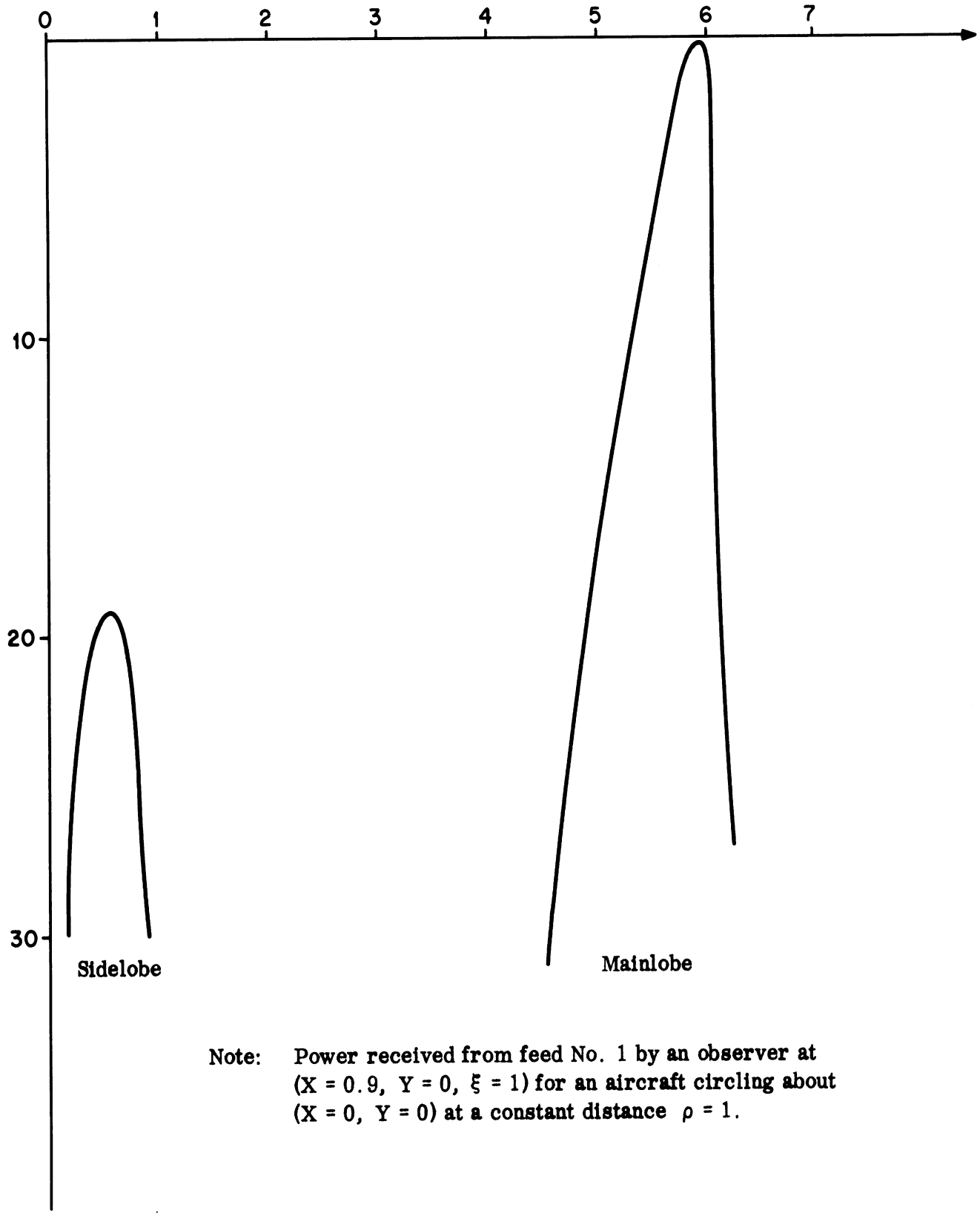

Note: Power received from feed No. 1 by an observer at ($X = 0.9$, $Y = 0$, $\xi = 1$) for an aircraft circling about ($X = 0$, $Y = 0$) at a constant distance $\rho = 1$.

FIG. 3-10: RECEIVED POWER AGAINST NORMALIZED TIME FOR AN AIRCRAFT CIRCLING ($\xi = 1$).

Therefore,

$$S = \frac{Vt}{z_a} = V\frac{t_o + \tau(t_o)}{z_a} = S_o + \frac{V}{c}\sqrt{S_o^2 + Y^2\left(\frac{2}{1+\xi}\right)^2} \quad . \qquad (3.15)$$

For the second case,

$$\tau(t_o) = \frac{z_a}{c}\sqrt{(\rho - Y_o)^2 \sin^2 S_o + \rho - (\rho - Y_o)\cos S_o}^2 + \left(\frac{2}{1+\xi}\right)^2 \quad . \qquad (3.16)$$

Therefore,

$$S \triangleq \frac{tV}{z_a} = S_o + \frac{V}{c}\sqrt{(\rho - Y_o)^2 + \rho^2 - 2\rho\,(\rho - Y_o)\cos S_o + \left(\frac{2}{1+\xi}\right)^2} \quad . \qquad (3.17)$$

For normal aircraft flight, V, of course, is much less than c, so that the normalized S may be approximately taken as S_o. For a closer estimate, we see that the AN/APN-153 antenna is pulsed, with pulse duration approximately equal to a few microseconds. Thus for the duration of a pulse, S_o is much smaller than Y, Y_o, or $\frac{2}{1+\xi}$, and can be neglected from the second terms in the expression for S (Eq. (3.15) and Eq. (3.17)). This implies that as far as the average power is concerned, we may neglect the change of time delay due to the motion of the airplane.* In other words the curves given by Fig. 3-3 and may be interpreted as illustrating the temporal variation of reflected radiation from a CW transmitter due to airplane motion. As a first approximation, for a pulsed transmitter, the intensity of the reflected radiation observed can be taken as the product of the two time functions, $P(t_o)$ and $M(t_o)$. In addition there will be a slight, and approximately constant shift of time scale given by Eq. (3.9) and (3.11).

---

* This approximation should be good for the duration that the reflected radiation is detectable by an observer. Thus, it is a reasonable approximation to apply when calculating radiated power. It is, of course, not valid when the frequency spectrum of the reflected radiation is under investigation.

3.3 Effect of Specularly Reflecting Clouds

To obtain an estimate of the effect of overcast on the doppler radiation observed at any point, we consider here a pessimistic case: that the cloud layer specularly reflects the radiation which reaches it. If the ground is also specularly reflecting, then the radiation observed at any point must consist of a sequence of rays representing the direct radiation, radiation reflected once from the ground, the radiation reflected from ground and bouncing back from the cloud, etc. Analytical expressions for these rays were given in the previous Radiation Laboratory Memorandum 01082-508-M. For the calculation of the power level of these multiple reflected rays, it is seen that the calculated data for the case of a specularly reflecting ground can be employed directing. In Fig. 3-11, the cloud layer is assumed to be of height z_c. Two rays are sketched:

1) The ray received by the observation point after a single reflection from the ground and

2) The ray received after reflection once from the ground and once from the cloud.

By the method of images, it is easy to see that the total radiation observed at any point may be considered as being due to an infinite set of sources (actually, sources and images) located at heights given by $z_a + 2nz_c$, $n = 0, 1, 2, 3 \ldots$, and their respective images.* In the previous discussion the calculation of direct radiation and ground reflection due to sources at any height are formulated. Hence the total radiation observed at any point can be obtained by summing up all the reflected components. For example, for an antenna and observation point configuration described by the normalized coordinates X, Y and ξ, the evaluation of the

---

* Theoretically, there is another set of image sources located at heights $2nz - z_a$, $n = 1, 2, 3 \ldots$ corresponding to rays reflected first from the cloud. However, for most normal operation of the radar, these components may be neglected because the beams are directed downwards.

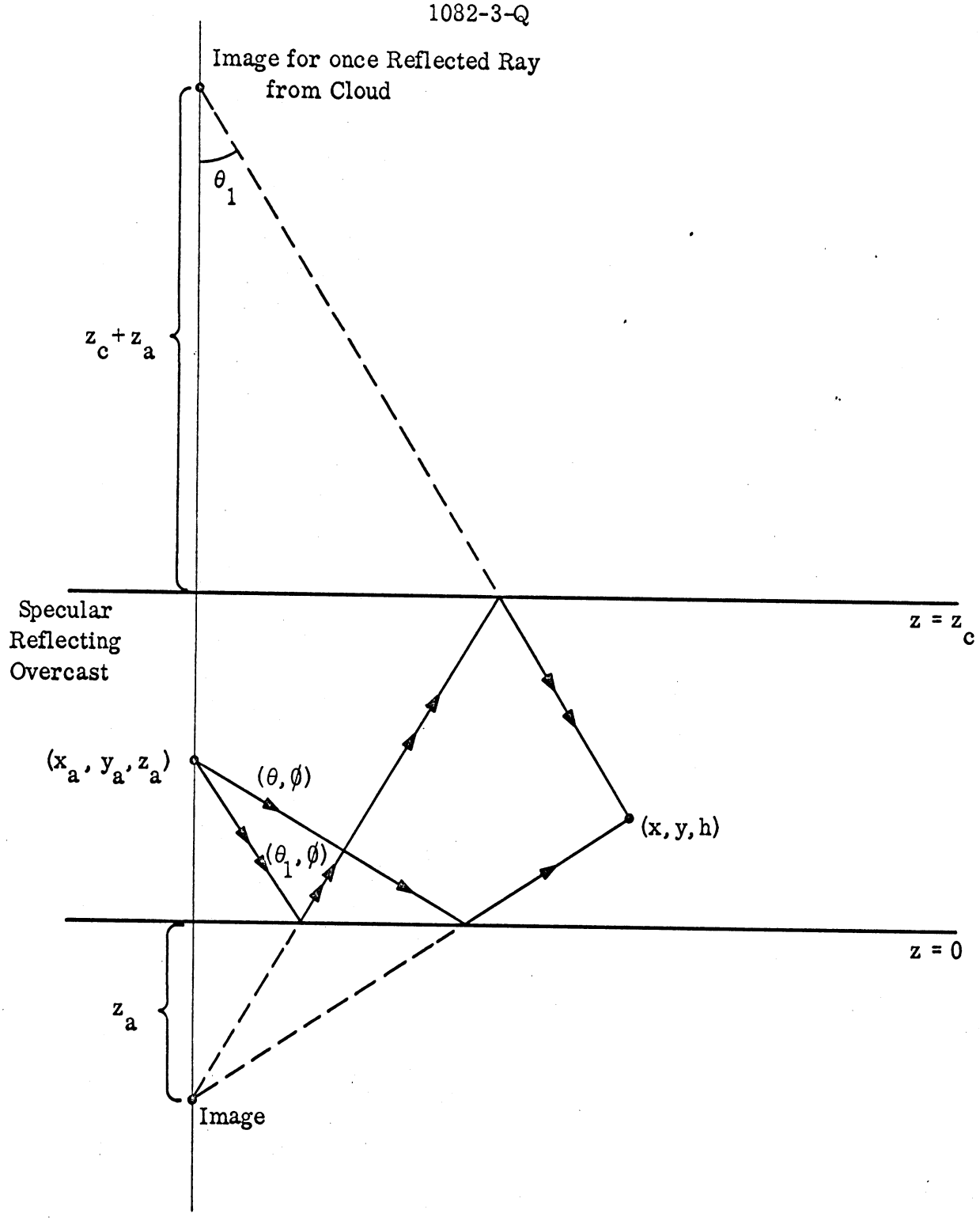

FIG. 3-11: GEOMETRY FOR SITUATION IN WHICH THERE IS SPECULAR REFLECTION FROM CLOUDS.

radiation from the various images can be obtained for the same X, Y by changing ξ. For a source at height $z_a + 2nz_c$, the value of ξ_n is given by

$$\xi_n = \frac{\left(\frac{2\xi}{\xi+1} + 2n\frac{z_c}{z_a}\right)}{\left(\frac{2}{\xi+1} + 2n\frac{z_c}{z_a}\right)} \quad . \tag{3.18}$$

In order to present an estimate of the power levels of the various orders of reflected rays the following case has been considered

$$X = 0.5$$

$$Y = 0$$

$$\xi = 0.817 \quad \text{or} \quad \frac{h}{z_a} = 0.1$$

and

$$\frac{z_c}{z_a} = 2 \quad .$$

In Fig. 3-12, the relative power levels of the direct and the reflected radiation are plotted against n. For the case of the curve marked "direct radiation", $n = 0$ corresponds to the directed radiation, and any order n corresponds to rays reflected n times from ground and cloud. For the case of the curve marked "ground reflected radiation", each order n corresponds to rays reflected $(n + 1)$ times from ground and n times from the cloud. The decrease in the power level with the multiplicity of reflection is to be expected.*

In practical cases, of course, the cloud and ground are not perfect reflectors. This fact may be accounted for by assuming a reflection coefficient Γ_g for the

*It should be noted that for some configurations (e.g., the observer "in line" with one of the multiple reflected rays which derives from the mainlobe) that the largest receiver power may occur for $n \neq 0$. These particular cases are at present being studied.

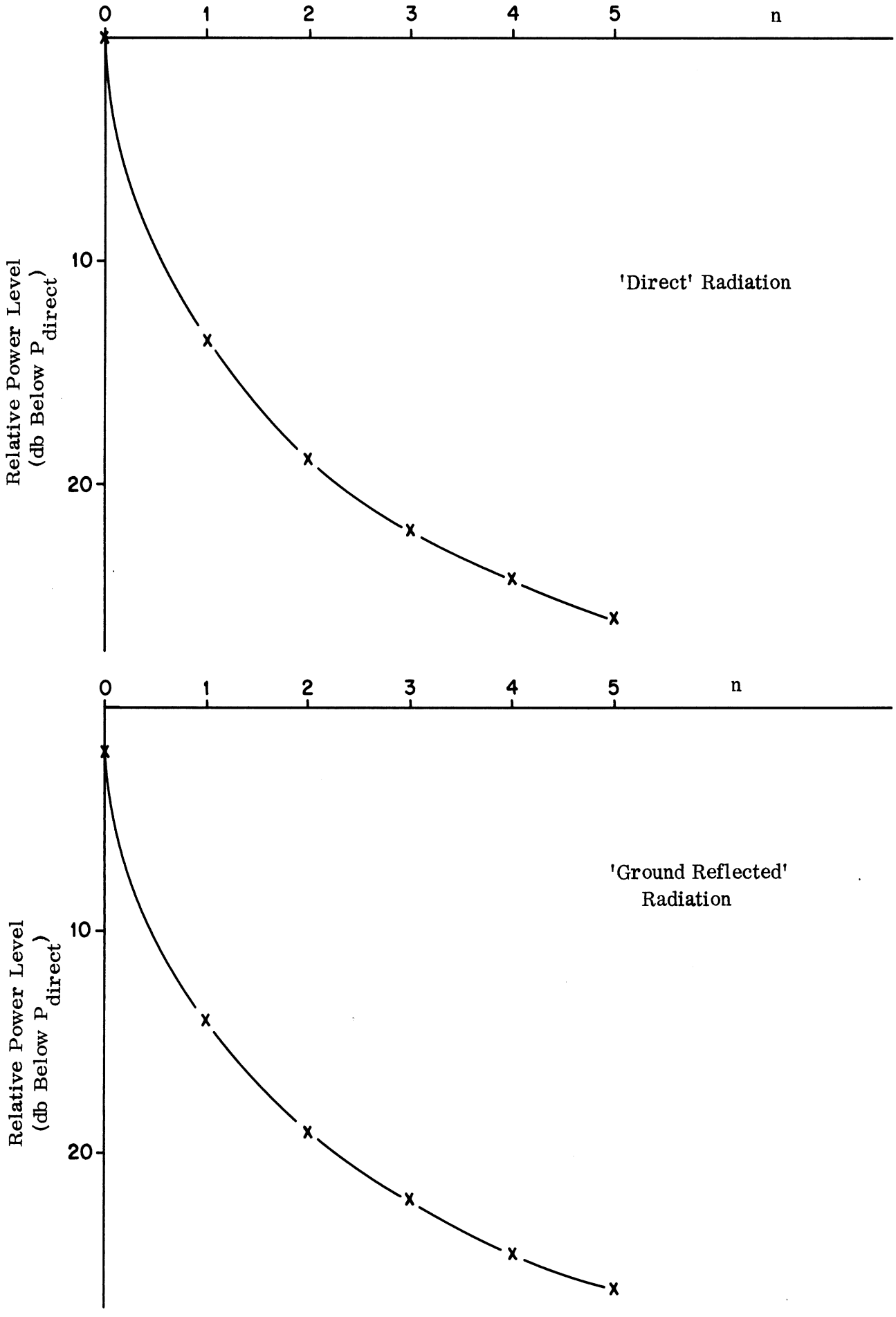

FIG. 3-12: RELATIVE POWER LEVEL FOR VARIOUS MODES OF REFLECTION.

ground and Γ_c for the cloud. Thus, the power level of each order of the "direct rays" should be modified by the factor $(\Gamma_g \Gamma_c)^n$ while those of the "reflected rays" should be modifed by the factor $\Gamma_g(\Gamma_g \Gamma_c)^{n+1}$. For reasonable values of $\Gamma_c \sim \Gamma_g \sim .6$, it is again obvious that when calculating the effect of clouds, only a few of the reflected waves need to be considered.

It is to be noted that the multiple reflected rays do not reach the point of observation at the same time. The time delay for each order of the "direct rays" is given by

$$t_n = \frac{z_a}{c}\sqrt{X^2 + Y^2 + \frac{2\xi_n}{1+\xi_n}} \tag{3.19}$$

while the time delay for each order of reflected rays is

$$t_n = \frac{z_a}{c}\sqrt{X^2 + Y^2 + \frac{2}{1+\xi_n}} \quad . \tag{3.20}$$

For the given example:

$$X = 0.5$$

$$Y = 0$$

$$\xi = 0.817$$

and

$$\frac{z_c}{z_a} = 2 \quad ,$$

the time delay for the various orders of reflected rays is given in Fig. 3-13.

3.4 Reflection from a Diffuse Ground

The reflected radiation due to a completely diffused ground observed at any point can be computed by integrating the power radiated from each part of the

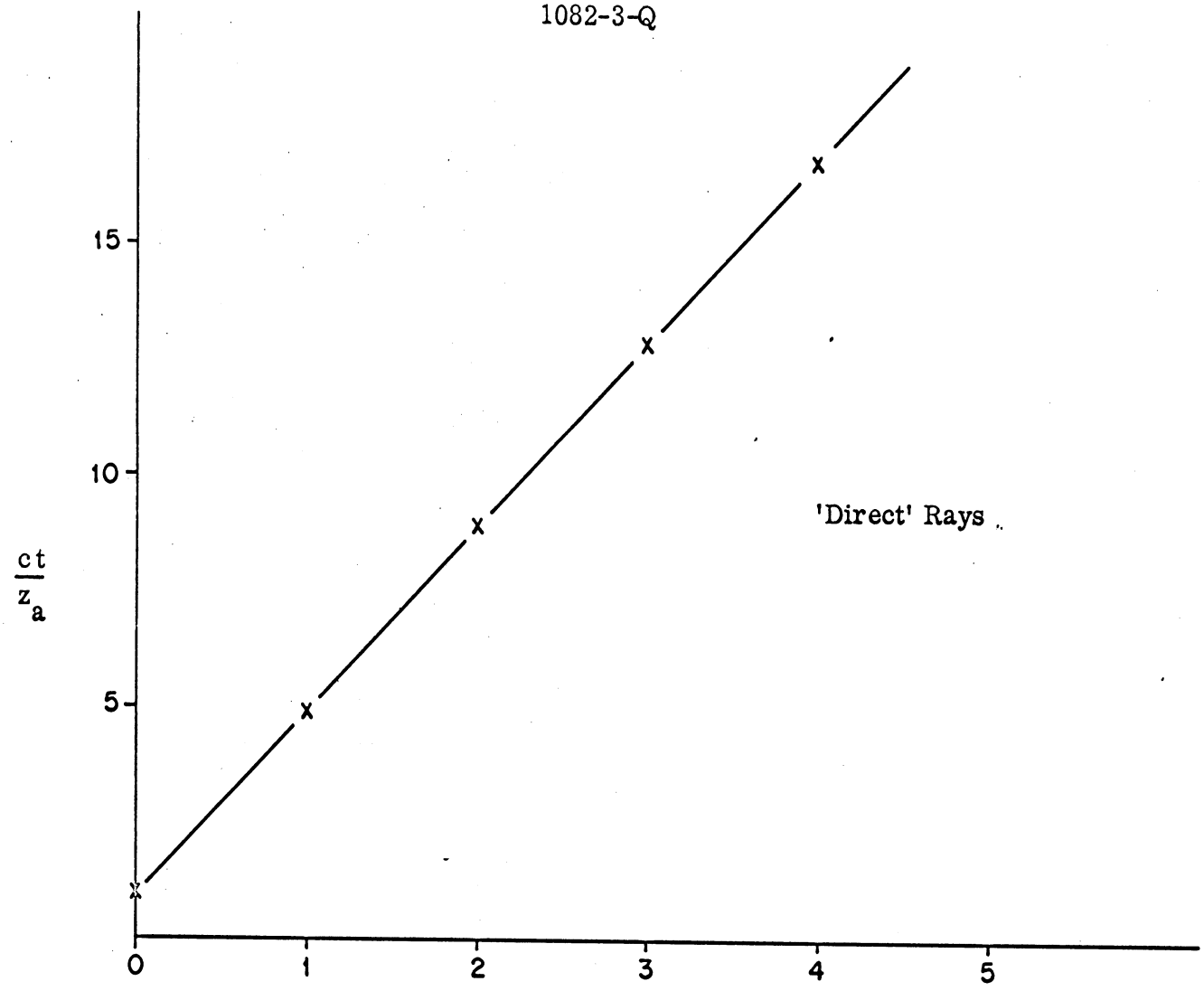

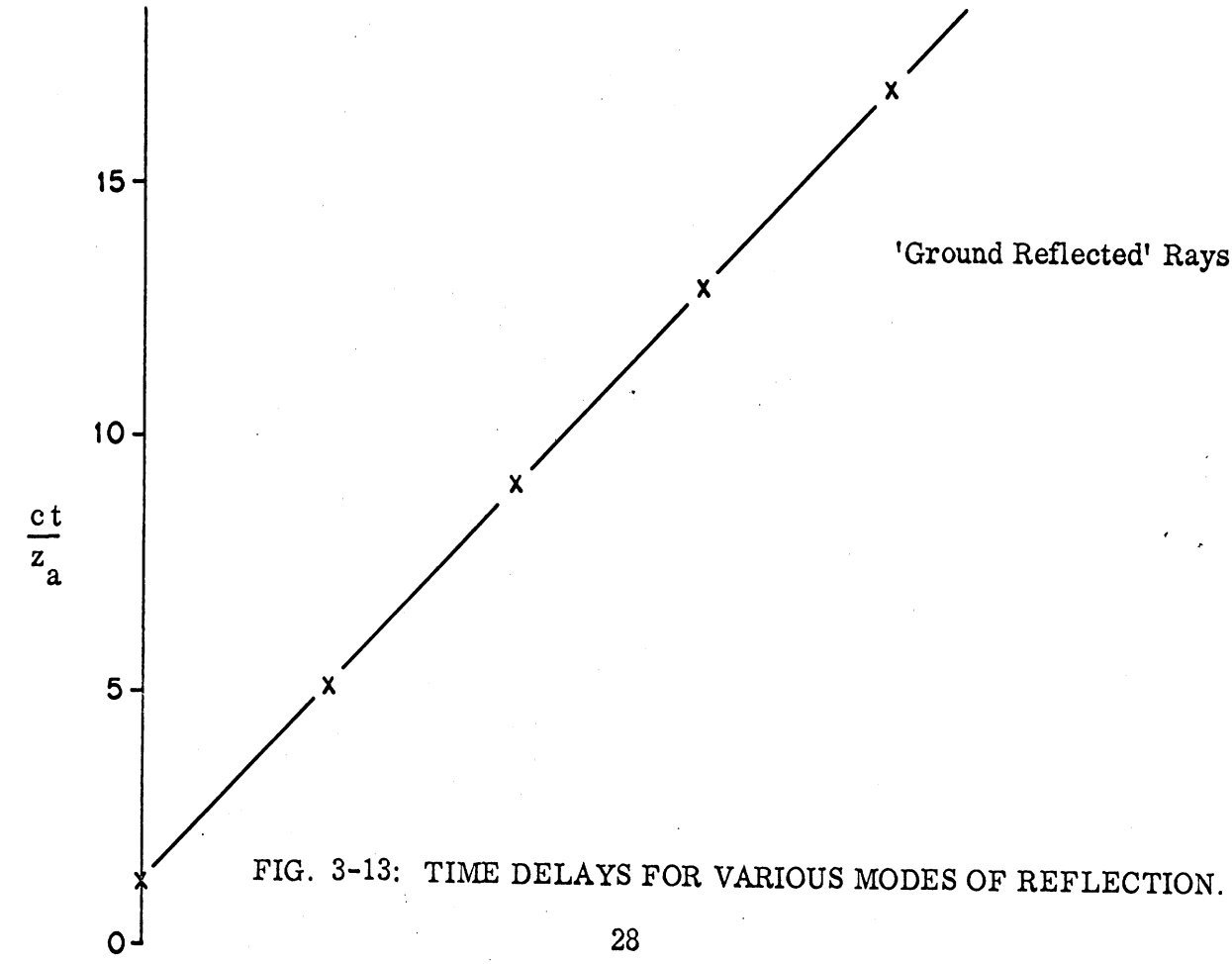

FIG. 3-13: TIME DELAYS FOR VARIOUS MODES OF REFLECTION.

ground. Referring to Fig. 3-14, it is seen that the power density of the direct radiation reaching the ground at a direction (θ, ϕ) from the antenna is,

$$S_d = \frac{P_t G_t f^2(\theta,\phi)}{4\pi z_a^2 \sec^2\theta} \quad . \tag{3.21}$$

For any signal radiated from the antenna t_o, the direct radiation will reach a part of ground as indicated by ΔA in Fig. 3-14 at a time t

$$t_d = t_o + \frac{z_a \sec\theta}{c} \quad . \tag{3.22}$$

From the geometry we have:

$$\Delta A = -z_a^2 \tan\theta \sec^2\theta \; \Delta\theta \; \Delta\phi \quad .$$

The power reflected by this elementary surface is

$$S_d \cos\theta \Delta A = -\frac{P_t G_t f^2(\theta,\phi)}{4\pi} \sin\theta \; \Delta\theta \; \Delta\phi \quad . \tag{3.23}$$

By the law of diffused reflection, this reflected power is uniformly distributed in the upper hemispherical region above ΔA, and would be observed at a point x_h, y_h, h at a time t_r given by

$$t_r = t_d + \frac{z_a}{c}\sqrt{(X-\tan\theta\cos\phi)^2 + (Y-\tan\theta\sin\phi)^2 + \left(\frac{1-\xi}{1+\xi}\right)^2} \quad . \tag{3.24}$$

The observed power density reflected from this elementary area is, therefore,

$$dS_r = \frac{P_t G_t f^2(\theta,\phi)\sin\theta\,\Delta\theta\,\Delta\phi\left(\frac{1-\xi}{1+\xi}\right)}{(8\pi)^2 z_a^2\left[(X-\tan\theta\cos\phi)^2 + (Y-\tan\theta\sin\phi)^2 + \left(\frac{1-\xi}{1+\xi}\right)^2\right]^{3/2}} \quad . \tag{3.25}$$

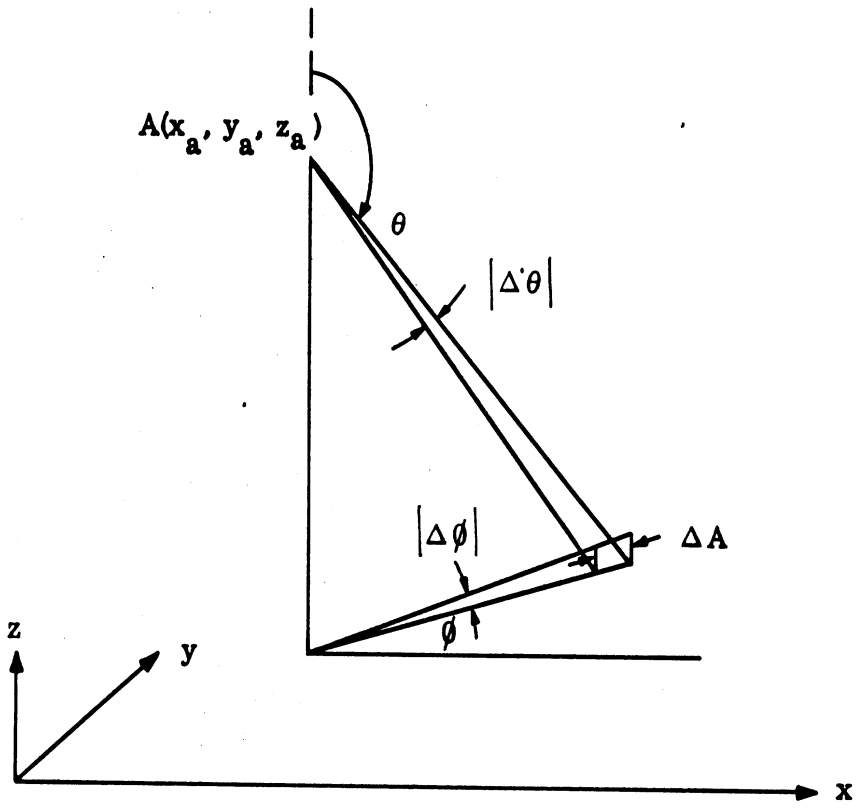

FIG. 3-14: GEOMETRY FOR DIFFUSE SCATTERING .

Due to the coordinate dependence of the time delay, a detailed analysis of the spatial and temporal variation of a pulsed signal from transmitter is extremely complicated. As a first approximation, based on a similar argument (but less coninvingly, perhaps) to that given in Section 3.2 we may investigate the power density of the reflected radiation observed at any point from a CW source, and use this result as the first order correction for the diffusely reflected power density from a moving, pulsed transmitter.

For a CW transmitter, the observed power density at any point may be obtained by integrating Eq. (3.25). The result is given by,

$$S_r(x_h, y_h, h) = -\frac{P_t G_t}{8\pi^2 z_a^2} \int_{\theta=\frac{\pi}{2}}^{\theta=\pi} d\theta \int_{\phi=0}^{\phi=2\pi} d\phi \cdot$$

$$\cdot \frac{f^2(\theta, \phi) \sin\theta \left(\frac{1-\xi}{1+\xi}\right)}{\left[(X - \tan\theta\cos\phi)^2 + (Y - \tan\theta \sin\phi)^2 + \left(\frac{1-\xi}{1+\xi}\right)\right]^{3/2}} \cdot \qquad (3.26)$$

If we write

$$S_r(x_h, y_h, h) = \frac{P_t G_t}{4\pi z_a^2} S_N(X, Y, \xi) \qquad (3.27)$$

a set of universal curves for S_N may be calculated for the radiation pattern of the transmitter, and may be referred to as the "pattern functions" of each antenna. Numerical calculations for the pattern functions of the antenna pattern of AN/APN-153 are currently being programmed and will be discussed in detail in the next report.

In our Memorandum 01082-508-M, we have considered the scattering from a model of rough surface which is not completely diffused, nor a Lambert surface

in the conventional sense. In that model, the surface is assumed to be composed of isotropic scatters that reflect radiation uniformly in all directions. For this model, it was shown that the power observed at any point, due to a CW source, and after scattering from the ground is given by

$$S_d = -\frac{P_t G_t}{(4\pi z_a)^2} \int_{\theta=\frac{\pi}{2}}^{\theta=\pi} d\theta \int_{\phi=0}^{\phi=2\pi} d\phi \cdot$$

$$\cdot \frac{f(\theta,\phi)\tan\theta}{\left[(X-\tan\theta\cos\phi)^2+(Y-\tan\theta\sin\phi)^2+(\frac{1-\xi}{1+\xi})^2\right]} \cdot \qquad (3.28)$$

Therefore the pattern function for this model is given by

$$S_N = \int_{\theta=\frac{\pi}{2}}^{\theta=\pi} d\theta \int_{0}^{\phi=2\pi} d\phi \cdot$$

$$\cdot \frac{f(\theta,\phi)\tan\theta}{\left[(X-\tan\theta\cos\phi)^2+(Y-\tan\theta\sin\phi)^2+(\frac{1-\xi}{1+\xi})^2\right]} \cdot \qquad (3.29)$$

The comparison of results derived from this "isotropic" model of the surface and the Lambert surface would of course yield some indication of the effect of the reflection properties of the surface on the intensity of the observed radiation.

Numerical results for the radiation reflected by the "isotropic" model of diffused surface for the antenna AN/APN-153 have been discussed in detail in the Memorandum 01082-508-M. Further results are given in Figs. 3-15 and 3-16.

To find the isotropically scattered power without resorting to a computer, an expression for the antenna pattern function must be assumed. In the progress

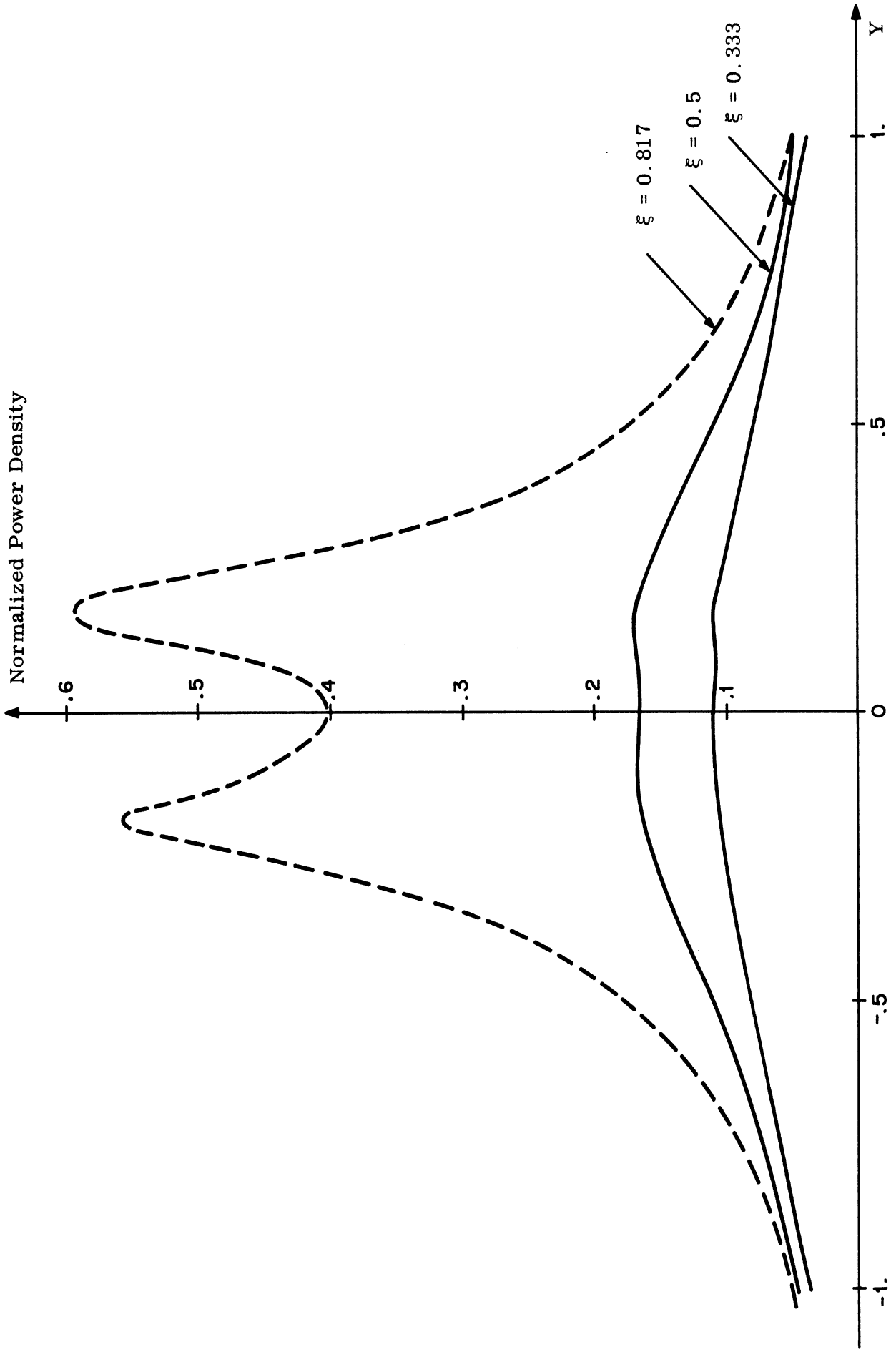

FIG. 3-15: RECEIVED POWER FROM FEED NO. 1 AFTER ISOTROPIC SCATTERING FOR X = 0.4 AND VARIOUS VALUES OF ξ.

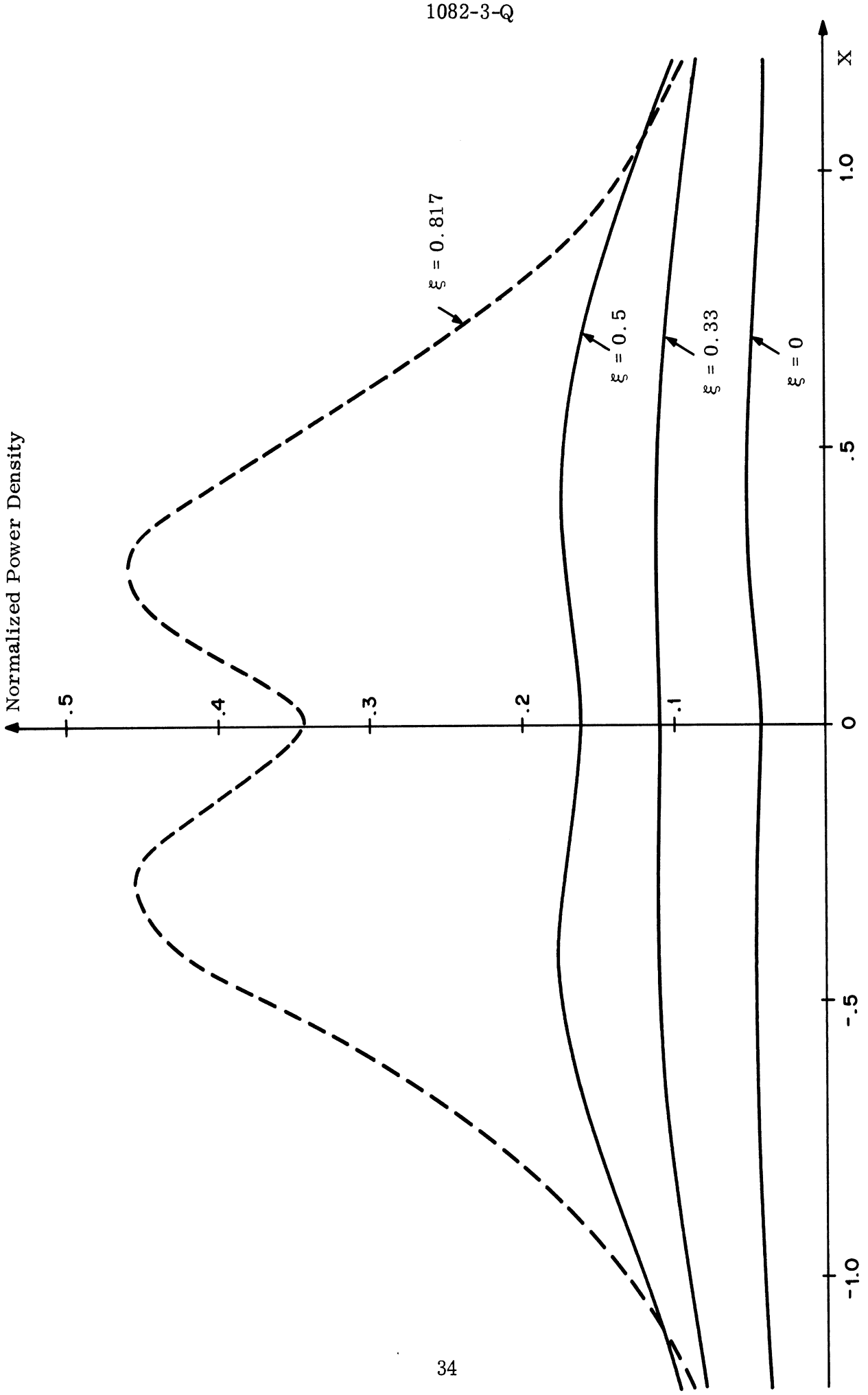

FIG. 3-16: RECEIVED POWER FROM FEED NO. 1 AFTER ISOTROPIC SCATTERING FOR Y = 0 AND VARIOUS VALUES OF ξ.

report, 1082-2-Q by Chu et al (1968) the Gaussian beam was introduced. For this case, Eq. (3.26) has the following form:

$$S_r(x_h, y_h, h) = -\frac{P_t G_t}{4\pi z_a^2} \int_{\alpha=\theta_a-\frac{3\pi}{2}}^{\theta_a-\frac{\pi}{2}} \int_{\beta=0}^{\beta=\pi} \cdot$$

$$\frac{e^{-\left[(a\alpha)^2+(b\beta)^2\right]} \sec^2(\theta_a-\alpha)\sec\theta_a \sec^2\beta \, d\alpha \, d\beta}{\left\{\tan^2(\theta_a-\alpha)+\sec^2\theta_a\tan\beta+1\right\}\left\{X^2+Y^2+\left(\frac{1-\xi}{1+\xi}\right)^2+\tan^2(\theta_a-\alpha)+\sec^2\theta_a\tan^2\beta-2X\psi_1-2X\psi_2\right\}} \tag{3.30}$$

where

$$\psi_1 \triangleq \tan(\theta_a-\alpha)\cos\phi_a - \sec\theta_a\tan\beta\sin\phi_a$$

and

$$\psi_2 \triangleq \tan(\theta_a-\alpha)\sin\phi_a + \sec\theta_a\tan\beta\cos\phi_a \quad .$$

The integral, Eq. (3.30), cannot be evaluated easily by hand unless some stronger restrictions are placed on the shape of the beam. If the beam is assumed thin, i.e., that a and b are large, then it is possible to assume that the exponential term dominates. Finally, we find that

$$S_N(X, Y, \xi) \triangleq \left(\frac{4\pi z_a^2}{P_t G_t}\right) S_r(x_h, y_h, h)$$

$$= \frac{\pi}{ab} \frac{\sec\theta_a}{\left\{X^2+Y^2+\left(\frac{1-\xi}{1+\xi}\right)^2+\tan^2\theta_a-2\tan\theta_a\left(X\cos\phi_a+Y\sin\phi_a\right)\right\}} \cdot \tag{3.31}$$

Figures 3-17 and 3-18 show the power received at fixed observation points in the direction of flight and in a direction perpendicular to the direction of flight. The corresponding curves obtained by numerical calculation are presented for comparison.

This type of approximate solution will, it is expected, be much better fit to the actual solution for narrower beams than that of the AN/APN-153.

Until we obtain the results for the power scattered by a diffuse ground, we will reserve making detailed comparison of these various curves.

3.5 Effect of Refractive Properties of Atmosphere

In the previous calculations of the radiation from a doppler radar system, the atmosphere is assumed to have the properties of free space. In practice, of course, the atmosphere has properties which vary with meteorological conditions and, in general it is stratified. Some dominant effects of meteorological conditions on the wave propagation considered in radar problems are:

1) The attenuation and scattering of radiation by precipitations and fog. Under these conditions there is an attenuation in the doppler signal which is returned to the antenna as well as in that seen by an observer. The scattering by precipitations and fog usually causes a change in the radiation spectrum. As far as the power level of radiation is concerned, the actual power returned to the aircraft or received by the observer must be multiplied by an appropriate attenuation function.

2) The stratification of the atmosphere, i.e., the variation of the refractive index of the atmosphere with height. Thus stratification of the atmosphere, causes the rays to be curved, and at times focussed with the result that a net change of the spatial distribution of the direct and ground reflected radiation occurs. Under extreme conditions, the gradient of the index refraction may cause the radiation to be guided along ducts and to be propagated over large distances without attenuation.

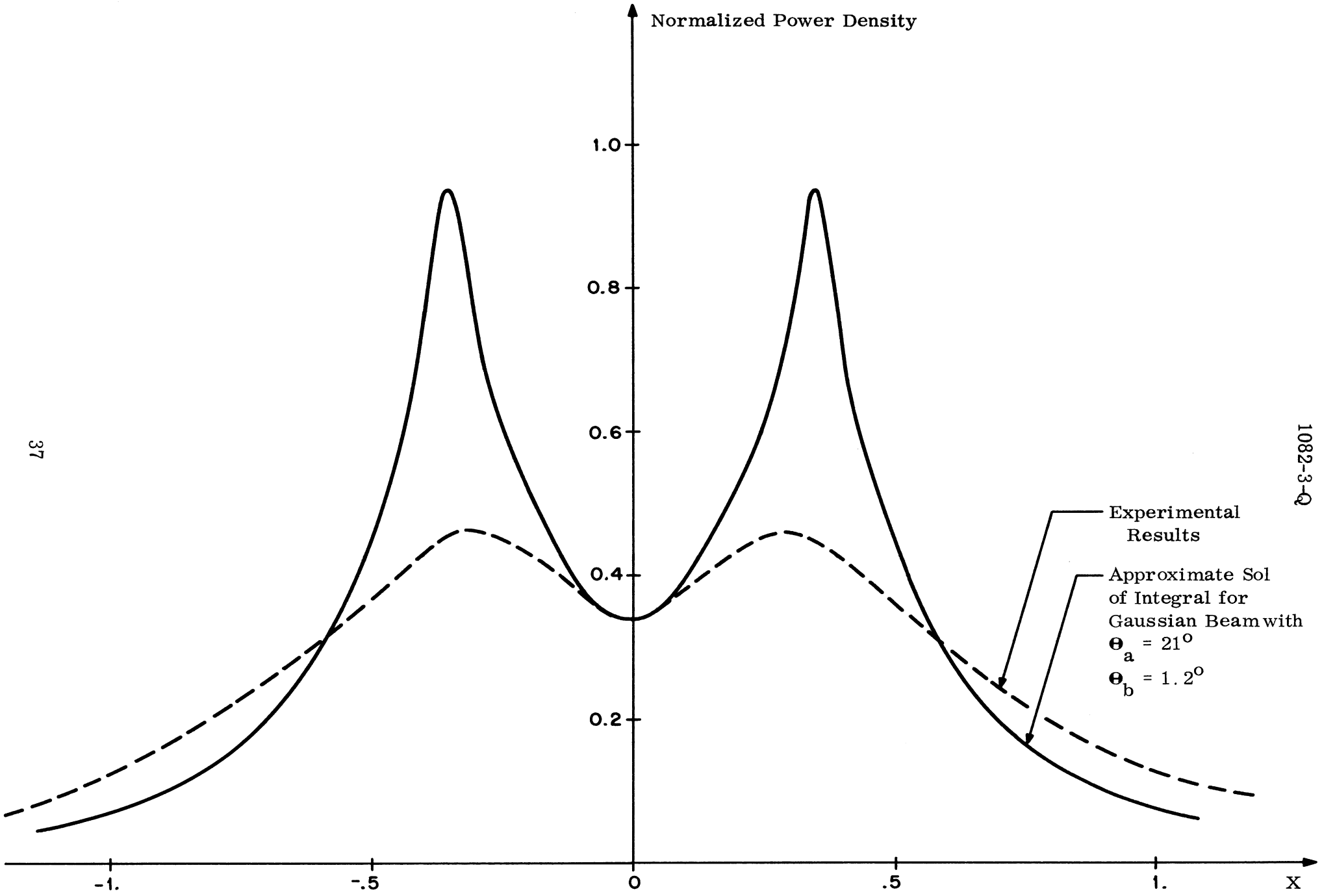

FIG. 3-17: NORMALIZED POWER DENSITY AFTER ISOTROPIC SCATTER FOR FEED NO. 1, Y = 0, $\xi = 0.817$ AGAINST X.

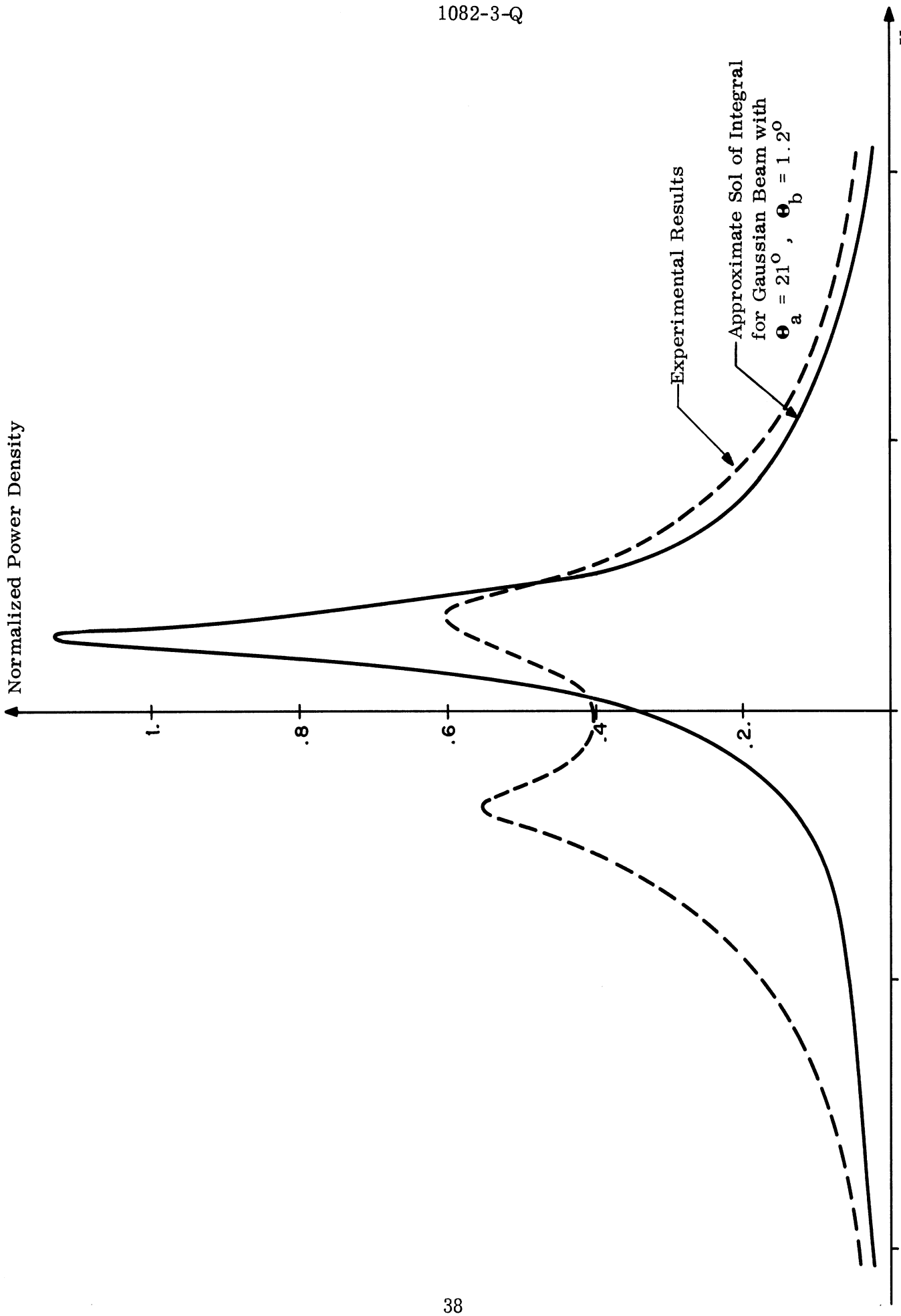

FIG. 3-18: NORMALIZED POWER DENSITY AFTER ISOTROPIC SCATTERING FOR FEED NO. 1, X = 0.4, ξ = 0.817.

A theoretical investigation of the effects of stratification primarily with application to doppler radiation has been started in this research period. Some mathematical deductions and approaches are outlined below.

It is well known that the refractive index of the atmosphere changes with height, due to changes of air density, pressure, temperature, etc. with height. For the standard atmosphere, the rate of change of atmospheric index of refraction, n, with height is about $-.039 \times 10^{-6}$ per meter (see NDRC report (1946)).

Over desserts and water a non-standard atmosphere is to be expected. The function $n(z)$, the refractive index profile, which describes the variation of refractive index with height must be used to characterize the atmosphere under such conditions. Further it is known that a discontinuity, or sudden change in the slope of $n(z)$, in general, causes some form of trapping or ducting effect.

Given an index profile $n(z)$, the differential equations for wave propagation may be written down. However an analytical solution for these equations, for arbitrary $n(z)$, are in general intractable. For high frequency propagation, the geometrical optics approach, or ray theory is adequate. For an account on the ray equation, and the amplitude variation along the ray in a stratified media, see Jones (1962). According to the ray theory, the field variation in the medium is approximately of the form:

$$P\, e^{i\frac{\omega}{c} L}$$

where P is the power density associated with the field, and $\frac{\omega}{c} L$ is the phase variation. The phase function L satisfies the Eikonal equation

$$\nabla L \cdot \nabla L = n^2 \tag{3.32}$$

and the power density satisfies the power conservation relation

$$\nabla \cdot [P \nabla L] = 0 \quad . \tag{3.33}$$

The radiation in a general media is primarily propagated along rays which are everywhere perpendicular to the surface of constant phase (or L). For a stratified media, differential equation may be derived from Eq. (3.32) and (3.33) to describe the ray path and the variation of L:

$$\frac{dx}{dz} = \frac{c_1}{\sqrt{n^2(z) - c_1^2 - c_2^2}} \tag{3.34}$$

$$\frac{dy}{dz} = \frac{c_2}{\sqrt{n^2(z) - c_1^2 - c_2^2}} \tag{3.35}$$

and

$$\frac{dL}{dz} = \frac{n^2(z)}{\sqrt{n^2(z) - c_1^2 - c_2^2}} \tag{3.36}$$

where c_1, c_2 are constant along a ray.

To investigate the effect of the stratification of atmosphere on the doppler radiation, we shall for convenience represent the function $n(z)$ by several broken straight lines, and investigate the change of ray path, power density, and the possibility of trapping for several slopes of $n(z)$.

We shall first consider the direct radiation, assuming that the antenna is at (z_a, y_a, z_a), and in an atmosphere characterized by

$$n(z) = n(z_a) + \rho(z - z_a) \tag{3.37}$$

where ρ is the slope of $n(z)$. Consider a ray starting from the antenna in a direction (θ, ϕ). If the atmosphere is uniform, the ray follows a straight line path as indicated in Fig. 3-19 (path I). Now is the atmosphere is stratified then from Eq. (3.37) we see that for this ray:

$$c_1 = n(z_a) \sin\theta \cos\phi \tag{3.38}$$

$$c_2 = n(z_a) \sin\theta \sin\phi \quad . \tag{3.39}$$

Equations (3.37) through (3.39) yield an expression for $n(z)$ which when substituted into Eqs. (3.34) and (3.35) give the following solutions for the ray path:

$$\left.\begin{matrix} x - x_a \\ y - y_a \end{matrix}\right\} = \frac{n(z_a)\sin\theta}{\rho} \left[\cosh^{-1}\left(\frac{n(z_a) + \rho(z - z_a)}{n(z_a)\sin\theta}\right) - \cosh^{-1}\left((\sin\theta)^{-1}\right)\right] \left\{\begin{matrix} \cos\phi \\ \cos\phi \end{matrix}\right\} .$$

For $\rho < 0$, the ray is curved toward the source, (path II in Fig. 3-19). On the other hand, for $\rho > 0$, the ray is curved upwards, (path III in Fig. 3-19).

This latter case is extremely undesirable in the operation of the doppler radar. In the first place, for some value of ρ and θ, the ray may be curved upwards without striking the ground, thus, causing a decrease or loss of the doppler signal. For a ray propagating from the antenna, the value of $n(z)$ decreases as the ray approaches the ground, provided $\rho > 0$. From Eq. (3.36) we find that the ray will not reach the ground unless

$$n(o) > n(z_a) \sin\theta \quad .$$

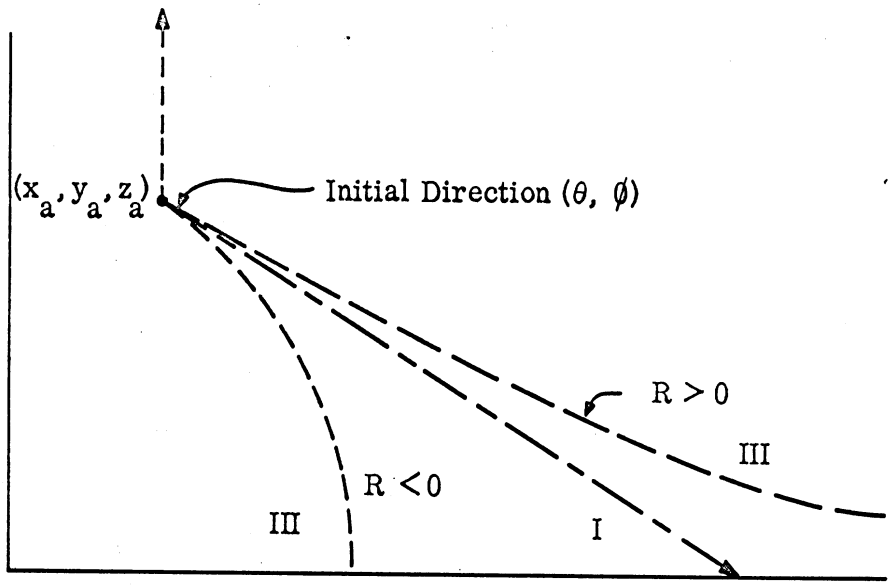

FIG. 3-19: RAY PATHS FOR A NON-CONSTANT REFRACTIVE INDEX.

Now the major portion of radiation is concentrated at $\theta \cong 20^{o}$. Thus, if the vehicle is in a region at which the refraction index is over four times that near the ground the ray will never reach the ground.

Furthermore for this case ($\rho > 0$), the reflected radiation is always traveling further, as evident from a comparison of rays II and III in Fig. 3-19. Numerical schemes for investigating how the profile gradient effects the detectability of doppler radiation will be continued in the next research period.

Extension of the analysis above, by considering $n(z)$ to be composed of two or three straight line segments of differing slopes, will give an indication of the possibility of ducts forming.

IV

TRIPS

Mr. Joseph E. Ferris visited the Canadian-Marconi organization in Montreal, Quebec, during the early part of March to discuss the systems being developed and produced by this organization. During this visit Mr. Haberl of Canadian-Marconi spent considerable time explaining and providing the visitor with information about systems being developed and the operation of Canadian - Marconi systems. Also during this visit pattern data for typical doppler systems was obtained. During the discussions it was learned that Canadian-Marconi does not make three-dimensional plots of their radiation patterns. However, they make an effort to obtain the two principal plane cuts and to evaluate the sidelobe levels and general pattern characteristics of their antenna on the basis of them. Their system operation is similar to that of the General Precision Laboratories (GPL) visited earlier by Mr. Ferris. Mr. Haberl expressed an interest in obtaining copies of our reports if they are available at the end of the contract. He felt it may be helpful to them in their future planning of the development of doppler systems.

REFERENCES

Atwood, S. S. (1946), "Radio Wave Propagation Experiments," Summary, Technical Report of the Committee on Propagation, NDRC, Washington, D.C., II.

Chu, C-M, J.E. Ferris and A.M. Lugg (15 January 1968), "Doppler Radiation Study," The University of Michigan Radiation Laboratory Report No. 01082-2-Q.

Jones, D.S. (1962), "High-Frequency Refraction and Diffraction in General Media," Phil. Trans. Royal Soc., 255, Series A, London.

Lugg, Andrew M. (1968), "Corrections to 1082-2-Q and a Outline of Work Completed Between January 15 through February 15, 1968," The University of Michigan Radiation Laboratory Memorandum No. 01082-508-M.

UNCLASSIFIED

Security Classification

DOCUMENT CONTROL DATA - R & D

(Security classification of title, body of abstract and indexing annotation must be entered when the overall report is classified)

1. ORIGINATING ACTIVITY *(Corporate author)*
The University of Michigan Radiation Laboratory, Dept. of Electrical Engineering, 201 Catherine Street, Ann Arbor, Michigan 48108

2a. REPORT SECURITY CLASSIFICATION
UNCLASSIFIED

2b. GROUP

3. REPORT TITLE

DOPPLER RADIATION STUDY

4. DESCRIPTIVE NOTES *(Type of report and inclusive dates)*
Quarterly Report No. 3 1 January 1968 - 1 April 1968

5. AUTHOR(S) *(First name, middle initial, last name)*

Chiao-Min Chu, Joseph E. Ferris and Andrew M. Lugg

6. REPORT DATE	7a. TOTAL NO. OF PAGES	7b. NO. OF REFS
April 1968	45	4

8a. CONTRACT OR GRANT NO.	9a. ORIGINATOR'S REPORT NUMBER(S)
N62269-67-C-0545	
b. PROJECT NO.	1082-3-Q
c.	9b. OTHER REPORT NO(S) *(Any other numbers that may be assigned this report)*
d.	

10. DISTRIBUTION STATEMENT

Requests for this document should be directed to NADC, Johnsville, Warminster, PA.18974

11. SUPPLEMENTARY NOTES	12. SPONSORING MILITARY ACTIVITY
	U.S. Naval Air Development Center Johnsville, Warminster, PA 18974

13. ABSTRACT

In this, the Third Quarterly Report on "Doppler Radiation Study", some results of the theoretical investigation and details of the experimental efforts are reported.

Much of the experimental work is directed toward preparing the equipment which will be used during the forthcoming fly-by tests. The radar tracking, data collection and communication equipment has been checked out and is ready for the scheduled test.

In the theoretical study, the numerical calculation of the spatial and temporal variation of the reflected radiation from a perfectly conducting ground, based on the scheme suggested in the last quarterly report, has been carried out. Further, some simplifications in presentation of the numerical results by using nomographs are introduced. The reflected radiation due to a diffusely reflecting ground is determined numerically and in an approximate but closed form; and finally the effect of some meteorogical conditions, such as cloud reflection, and the variation of the refractive index of the atmosphere are also considered.

DD FORM 1 NOV 65 1473

UNCLASSIFIED

Security Classification

14. KEY WORDS	LINK A		LINK B		LINK C	
	ROLE	WT	ROLE	WT	ROLE	WT
DOPPLER NAVIGATIONAL SYSTEMS						
AIRBORNE RADAR						
RADIATION PATTERNS						
GEOMETRICAL OPTICS						